npj | precision oncology

Article

Published in partnership with The Hormel Institute, University of Minnesota

https://doi.org/10.1038/s41698-025-01166-3

KRAS-targeted therapies in colorectal cancer: a systematic analysis of mutations, inhibitors, and clinical trials

Maria Navarro-Jiménez[1,4,5], Beatriz González[1,5], Nuria Mulet[2,3], Cinta Hierro[2,3] & Sergio Alonso[1] ✉

KRAS mutations occur in over one-third of colorectal cancers (CRC), primarily affecting codons 12 and 13, and less frequently codons 61, 117, and 146. Rare mutations in other codons have been reported, but often lack clear functional significance. These mutations activate pathways that drive cell proliferation, impair differentiation, and suppress apoptosis. *KRAS*-mutant CRCs are associated with poorer prognosis, higher recurrence rates, reduced chemotherapy response, and resistance to EGFR-targeted therapies. Stratifying patients by *KRAS* mutation status is now standard for guiding treatment, though not all mutations confer the same oncogenicity or therapeutic response. Once considered undruggable, recent advances have led to the development of inhibitors targeting specific *KRAS* mutant isoforms. Consequently, precise characterization of *KRAS* mutational profiles is critical to optimize treatment strategies in CRC. This study provides a systematic analysis of *KRAS* mutation frequency and co-occurrence, reviews current targeted therapies, and examines ongoing clinical trials for the most prevalent *KRAS* alterations in CRC.

Colorectal cancer (CRC) is the third most common and the second most lethal human cancer, with a worldwide incidence of nearly 2 million cases and close to 1 million deaths annually[1]. Most CRCs arise through a sequential process initiated by mutations in genes controlling cell division, leading to uncontrolled proliferation and the development of benign polyps. These lesions can progress to malignancy through the acquisition of additional genomic alterations, including chromosomal abnormalities, genetic mutations, and epigenetic modifications in genes regulating proliferation, differentiation, apoptosis, and angiogenesis[2].

CRC comprises a heterogeneous group of tumors with distinct mutational profiles and phenotypic characteristics. Following the discovery of the mutator phenotype in the early 1990s, CRCs have been classified clinically into two main categories: microsatellite-stable (MSS) tumors, proficient for mismatch repair systems (pMMR), and tumors with microsatellite instability (MSI), characterized by deficiencies in mismatch repair systems (dMMR) leading to a prominent mutator phenotype primarily targeting microsatellite sequences[3]. This classification has been fundamental for understanding CRC etiology and biology, as well as for clinical management.

In 2012, the Cancer Genome Atlas (TCGA) consortium published a comprehensive molecular analysis of CRCs, classifying tumors into two main groups based on somatic mutation rate: non-hypermutated tumors (mostly MSS) and hypermutated tumors, mainly comprising MSI and tumors with mutations in the DNA polymerase epsilon gene, *POLE*[4]. The TCGA study epitomized decades of research, providing strong evidence of the molecular heterogeneity of CRC and the distinct nature of hypermutated (MSI and *POLE* +) versus non-hypermutated cancers. In 2015, an alternative classification system comprising four molecular subtypes, based on transcriptomic profiling, was proposed[5]. While this transcriptome-based classification correlates with tumor characteristics and patient outcomes, it has not yet been widely adopted in clinical practice.

Ras proteins are small GTPases functioning as molecular switches that activate fundamental signal transduction pathways regulating cell growth, differentiation, and apoptosis. Humans possess three RAS genes—*HRAS*, *KRAS*, and *NRAS*—encoding four proteins (*KRAS* encodes two splicing variants, *KRAS4A* and *KRAS4B*) with high sequence similarity[6]. Despite this, RAS isoforms differ in tissue distribution, membrane localization, and downstream signaling preferences, contributing to distinct mutation spectra and oncogenic roles across tumor types.

[1]Cancer Genetics and Epigenetics Group (CGE), Translational Program in Cancer Research (CARE), Germans Trias i Pujol Research Institute (IGTP), Badalona, Spain. [2]Department of Medical Oncology, Institut Català d'Oncologia (ICO) Badalona, Badalona, Spain. [3]Badalona Applied Research Group in Oncology (B-ARGO), Badalona, Spain. [4]Present address: Ability Pharmaceuticals, SA Cerdanyola del Vallès, Barcelona, Spain. [5]These authors contributed equally: Maria Navarro-Jiménez, Beatriz González. ✉e-mail: salonsou@igtp.cat

RAS proteins cycle between an active, GTP-bound state and an inactive, GDP-bound state. Activation occurs upon stimulation by growth factors interacting with membrane-bound receptors, leading to signal transduction via GRB2 and SOS (a guanine-exchange factor, GEF), which catalyze GDP-GTP exchange and activate Ras. This conformational change is detected by Ras effectors, activating downstream pathways, most notably RAF/MEK/ERK (MAPK pathway) and PI3K/AKT/mTOR (PI3K pathway), regulating apoptosis suppression, cell growth, transformation, migration, and differentiation[7]. Ras is inactivated through the hydrolysis of GTP to GDP, catalyzed by the intrinsic GTPase activity of Ras and accelerated by GTPase-activating proteins (GAPs). The most prominent RAS GAPs are neurofibromin 1 (NF1) and RASA1 (also known as p120GAP).

The mutation frequency and profile vary across cancer types and *RAS* genes, illustrating that not all *RAS* mutations are equal and that specific mutations exhibit unique biological and clinical behaviors[8]. The forces that drive specific mutations in *RAS* genes to dominate over others result from a complex interplay of factors, including tissue-specific aspects such as genotoxic stress, biological selection, genomic topology, gene expression, and cellular context[9,10]. The most common cancer-related Ras alterations are missense mutations disrupting the balance between inactive and active forms, typically involving amino acid substitutions that decrease GTP hydrolysis or increase GTP loading[6]. Mutations at codons 12, 13, 61, and 146 disrupt GAP-mediated GTP hydrolysis, leading to constitutive Ras activation and persistent downstream signaling, promoting cell survival and uncontrolled proliferation. The mutated amino acid determines both the biochemical activity and transforming capacity of mutant KRAS[9]. Cells harboring different *KRAS* mutations also differ in glycolysis, glutamine usage, and amino acid, choline, and nucleotide hexosamine metabolism, potentially influencing responses to anticancer treatments[11].

Inhibitors targeting proteins upstream and downstream of KRAS in the MAPK and PI3K pathways have long been approved for clinical use[12,13]. However, developing specific KRAS inhibitors faced significant challenges due to the picomolar affinity of KRAS for GTP/GDP, high intracellular GTP concentrations, lack of allosteric regulatory sites, and the complex network of interactions involving GEFs, GAPs, and effectors through extended protein-protein interaction surfaces that are inherently challenging to target by small molecules[14]. Overcoming the picomolar affinity of RAS for GTP would require the development of small molecules with exceptional binding properties, largely surpassing those of ATP-binding protein inhibitors. Furthermore, the GTP-binding pocket varies among KRAS mutations, complicating inhibitor design[15]. Due to repeated failures of both direct and indirect approaches, KRAS was long considered "undruggable." The development of sotorasib and adagrasib, *KRAS* G12C-specific inhibitors, redefined KRAS as a challenging but tractable target, leading to an unprecedented surge in KRAS-targeted therapies in the last few years[16].

Over the years, new strategies to inhibit KRAS signaling have emerged, focusing on: (i) inhibitors targeting oncogenic mutant *KRAS* isoforms, (ii) disruption of KRAS-effector interactions to prevent downstream signaling, (iii) inhibition of KRAS/GEF interactions to prevent GTP recharge[17]. In addition, vaccines (peptide-based and mRNA) and T-cell receptor (TCR)-engineered T-cell therapies are currently under development for *KRAS*-mutated cancers[18].

The *KRAS* G12C inhibitors sotorasib and adagrasib, which covalently bind to the cysteine-12 residue of mutant KRAS, were the first to gain regulatory approval following advanced clinical development[19,20]. These inhibitors block *KRAS* G12C in its inactive GDP-bound state, preventing SOS-catalyzed nucleotide exchange and downstream signaling. However, they do not affect wild-type or other frequent KRAS mutants lacking cysteine in the active site. Many KRAS G12C inhibitors with similar mechanisms are in clinical development[15].

KRAS G12C inhibitors have shown remarkable success in cancers harboring the G12C mutation, but as they are designed explicitly for this allele, they are not active against more prevalent *KRAS* mutations such as G12D and G12V. In 2021, Wang et al.[21] reported the first KRAS G12D-targeting inhibitor, MRTX1133, which binds the switch II pocket of KRAS, inhibiting both active and inactive states. MRTX1133 is highly selective for KRAS G12D and induces tumor regression in multiple in vivo models, including CRC[22]. Since then, numerous molecules have been developed to target the most common G12D and G12V KRAS mutants.

Pan-RAS inhibitors target both wild-type and mutant forms of all RAS proteins, including KRAS, NRAS, and HRAS, offering broader applicability and the ability to potentially block compensatory activation or secondary mutations in *KRAS*, *NRAS*, or *HRAS* after initial KRAS inhibition. However, simultaneous inhibition of all three RAS isoforms in normal cells carries a serious risk of toxicity[23].

Pan-RAS inhibitors follow several possible strategies: (i) direct inhibition of Ras proteins, such as RMC-6236 (daraxonrasib), a multi-RAS(ON) inhibitor capable of inhibiting multiple Ras isoforms, including any mutation in *KRAS*, *NRAS*, and *HRAS*, and the wild-type isoforms[24]; (ii) indirect Ras targeting by inhibiting SOS1-driven GDP/GTP exchange, such as BI 1701963. SOS1 inhibitors are often combined with other KRAS inhibitors to suppress feedback reactivation and enhance response[25].

First-generation KRAS inhibitors, including sotorasib and adagrasib, exclusively target the GDP-bound inactive form (OFF). Treatment with these inhibitors often triggers an adaptive feedback reactivation of wild-type RAS-GTP or secondary mutations promoting tumor persistence[26,27]. RAS(ON) inhibitors, which target the GTP-bound active form, have demonstrated superior efficacy. Revolution Medicines has developed a class of RAS(ON) inhibitors that stabilize a ternary complex between mutant KRAS, a chaperone protein, and the inhibitor, exploiting chaperone-assisted conformational changes to create a druggable pocket. This complex sterically blocks KRAS-effector interactions, inhibiting downstream signaling. Examples of these inhibitors include RMC-6291 (elironrasib, KRAS G12C), RMC-4998 (KRAS G12C), RMC-9805 (zoldonrasib, KRAS G12D), RMC-5127 (KRAS G12V), RMC-8839 (KRAS G13C), and RMC-0708 (KRAS Q61H). In addition, RAS(ON) inhibitors such as RMC-7977 and RMC-6236 exhibit broader activity, targeting multiple mutant and wild-type RAS isoforms and overcoming resistance commonly observed with RAS-OFF inhibitors[24,28]. Preclinical studies show sustained suppression of RAS pathway signaling and prolonged tumor regression, whereas RAS(OFF) inhibitors often lead to relapse due to adaptive resistance[29].

In addition to pharmacological inhibition of KRAS, immunotherapeutic approaches for *KRAS*-mutant cancers—including vaccines and adoptive T-cell therapies—are currently in development. Peptide vaccines targeting KRAS were tested long ago[30,31], but single peptides often fail to produce adequate epitopes for sufficient T-cell activation. DNA vaccines targeting KRAS have also been explored[32]. Individualized mRNA-based vaccination has recently been used in patients with non-small cell lung cancer (NSCLC), CRC or pancreatic adenocarcinoma with *KRAS* mutations[22,33]. For instance, mRNA-derived KRAS-targeted vaccine V941 (mRNA-5671) is based on a lipid nanoparticle (LNP)-formulated mRNA that targets four of the most prevalent *KRAS* mutations (G12D, G12V, G12C and G13D). Currently, most KRAS-targeting immunotherapeutic strategies remain in early stages of development, and none have yet advanced to clinical application.

Therapeutic strategies for KRAS-mutant metastatic colorectal cancer (mCRC) are increasingly moving beyond single-agent KRAS inhibition. Combining KRAS inhibitors with anti-EGFR therapy or other targeted agents has emerged as a promising approach, as it can enhance antitumor efficacy compared with KRAS inhibition alone. This combination strategy is based on the principle of vertical or parallel pathway blockade: by simultaneously targeting multiple proteins within the MAPK signaling cascade or complementary pathways, it would be possible to reduce compensatory signaling and delay the emergence of resistance mechanisms that frequently limit the durability of monotherapy. Recent preclinical and clinical studies have demonstrated the potential of these combination approaches to improve response rates and progression-free survival in patients with *KRAS*-mutant cancer[26,34,35]. These observations underscore the importance of rational combination strategies in the development of precision therapies for this challenging patient subgroup.

Table 1 | Clinical and pathological characteristics of the CRC datasets used in this study

	DFCI	TCGA	MSK Primary	MSK Metastases	*p*-value
Number of samples	619	528	601	532	
Biological Sex					
Female	380 (61%)	254 (48%)	277 (46%)	241 (45%)	6.5×10^{-9}
Male	239 (39%)	274 (52%)	324 (54%)	291 (55%)	
Age at diagnosis (mean±s.d.)	70.7 ± 8.6	65.8 ± 13.0	55.2 ± 13.3	54.0 ± 12.2	$<2 \times 10^{-16}$
Stage at diagnosis					
Stage I	152 (25%)	96 (18%)	21 (3%)	20 (4%)	$<2 \times 10^{-16}$
Stage II	187 (30%)	203 (39%)	80 (13%)	53 (10%)	
Stage III	159 (26%)	157 (29%)	147 (24%)	127 (24%)	
Stage IV	65 (11%)	72 (14%)	353 (59%)	332 (62%)	
N.D.	56 (9%)	0	0	0	
MSS vs. MSI/Hypermutated					
MSS	496 (80%)	432 (82%)	504 (84%)	513 (97%)	1.7×10^{-15}
MSI or Hypermutated	123 (20%)	96 (18%)	97 (16%)	19 (3.6%)	

p-values were calculated using Fisher's exact test for contingency tables, except for age at diagnosis that was analyzed by ANOVA.

The clinical utility of KRAS-targeted therapies in CRC depends on the specific distribution of *KRAS* mutations and their co-occurrence with other genetic alterations. Numerous publications have explored the incidence of *KRAS* mutations in CRC, some of them analyzing a very large number of samples[36,37]. Resources like the Catalog Of Somatic Mutations In Cancer (COSMIC)[38], provide invaluable tools to explore mutational profiles across large samples, but aggregation studies may introduce biases due to varying sample selection and mutation-detection strategies (e.g., targeted sequencing, whole-exome sequencing, or whole-genome sequencing). These resources also do not always provide information about critical factors affecting *KRAS* mutation incidence, such as mismatch repair deficiencies or *POLE* mutations leading to a hypermutator phenotype.

Given the diversity of *KRAS* mutations and their emerging therapeutic relevance, a deeper understanding of their incidence, co-mutation patterns, and response to targeted therapies in CRC is needed. In this study, we present a detailed analysis of the *KRAS* mutational profile in three large CRC cohorts with comprehensive clinical and mutational data, correcting for factors known to influence *KRAS* mutation incidence. We also examine how different *KRAS* mutations and their co-mutated genes may impact therapeutic strategies for CRC patients, taking into account the most up-to-date status of active clinical trials evaluating KRAS-targeted therapies in CRC. Our discussion addresses both approved treatments and those currently under clinical investigation.

Results

Incidence of RAS mutations in colorectal cancer

According to the data from COSMIC, *KRAS* is the most frequently mutated oncogene in CRC, with an incidence of 34% in adenocarcinomas originating from the large intestine[38]. In contrast, mutations in *NRAS* and *HRAS* occur at much lower frequencies, accounting for 4% and 1% of cases, respectively. However, the COSMIC database compiles data from very heterogeneous studies, with different patient selection criteria and mutation analysis methodology, which may bias the observed mutational frequencies. To obtain a more accurate estimation of *RAS* mutations frequency in CRC, we conducted a comprehensive analysis across the largest colorectal cancer cohorts from cBioportal[39]: DFCI (primary CRCs from Dana Farber Cancer Institute)[40], TCGA Pancancer (primary CRCs from the Cancer Genome Atlas consortium)[41] and MSKCC (primary CRCs and metastases from Memorial Cancer Sloan Kettering Cancer Center)[42] (see "Methods"). There were substantial differences in demographic, clinical, and pathological characteristics of the patients from these three cohorts that were taken into account for the subsequent analyses (Table 1).

Association of RAS mutations with tumor stage, MSI status and cohort

KRAS was mutated in 38% (670/1748) of the primary CRCs, while *NRAS* and *HRAS* exhibited considerably lower mutation incidence (4.9%, 85/1748, and 0.9%, 15/1748, respectively). Mutational frequencies were similar in metastases, i.e., *KRAS* (41%, 216/532), *NRAS* (3.9%, 21/532), and *HRAS* (0.4%, 2/532), with no statistically significant difference compared to primary tumors (Fig. 1). The similar mutational incidence between primary tumors and metastases was consistent with the general view that *RAS* mutations are early events in CRC and, importantly, that mutations in these genes do not have a substantial effect in metastatic progression. In contrast, other genes frequently mutated in CRC, such as the tumor suppressors *APC, TP53, FBXW7*, and *SMAD4*, and the oncogenes *PIK3CA* and *BRAF* exhibited statistically significant differences in mutation frequency when comparing primary tumors vs. metastasis (Fig. 1 and supplementary Fig. S1).

In primary tumors, *KRAS* mutations were more frequent in MSS than in MSI/hypermutated cancers (40% vs. 31%, OR = 0.7, CI = [0.5–0.9], $p = 0.002$, Fisher's exact test) while *HRAS* mutations strongly associated with MSI/hypermutated cancers (3.8% vs. 0.2%, OR = 18.7, 95%CI = [5–104], $p = 2.7 \times 10^{-7}$, Fisher's exact test) (Fig. 1). *KRAS* mutations were more frequent in advanced tumors (Stage III/IV, 399/955, 41.8%) than in Stage I/II tumors (253/743, 34.1%, $p = 0.001$, Fisher's exact test). *NRAS* and *HRAS* exhibited similar mutational frequencies in Stage I/II vs. Stage III/IV primary tumors. Multivariable logistic regression including biological sex, MSI status, tumor stage and cohort, confirmed the association of *KRAS* mutations with MSS tumors (OR = 1.4, CI = [1.1–1.8], $p = 0.014$) and *HRAS* with MSI tumors (OR = 15.7, CI = [5.0–48.8], $p = 2 \times 10^{-6}$) (Fig. 1B). Of note, most *HRAS* mutations (88%, 15/17) were in codons outside of G12, G13, Q61, K117, and A146, suggesting uncertain oncogenic potential and a likely passenger role. Multivariable logistic regression analysis revealed that *KRAS* mutations were more frequent in the TCGA (OR = 1.8, CI = [1.4–2.5], $p = 4 \times 10^{-6}$) and MSKCC (OR = 2.2, CI = [1.6–3.0], $p = 1.6 \times 10^{-8}$) cohorts in comparison to the DFCI cohort. This difference was not explained by differences in biological sex, MSI or stage among the different cohorts (Fig. 1B). Similar multivariable analyses on the most frequently mutated genes revealed significant differences in mutational frequencies in *APC, TP53, PIK3CA* and *BRAF* among cohorts (Supplementary Fig. S1).

Concordance of KRAS mutations in tumor samples from the same patients

The MSKCC dataset comprised 31 cases where more than one tumor sample was analyzed (supplementary Fig. S2). In 19 of them, at least one

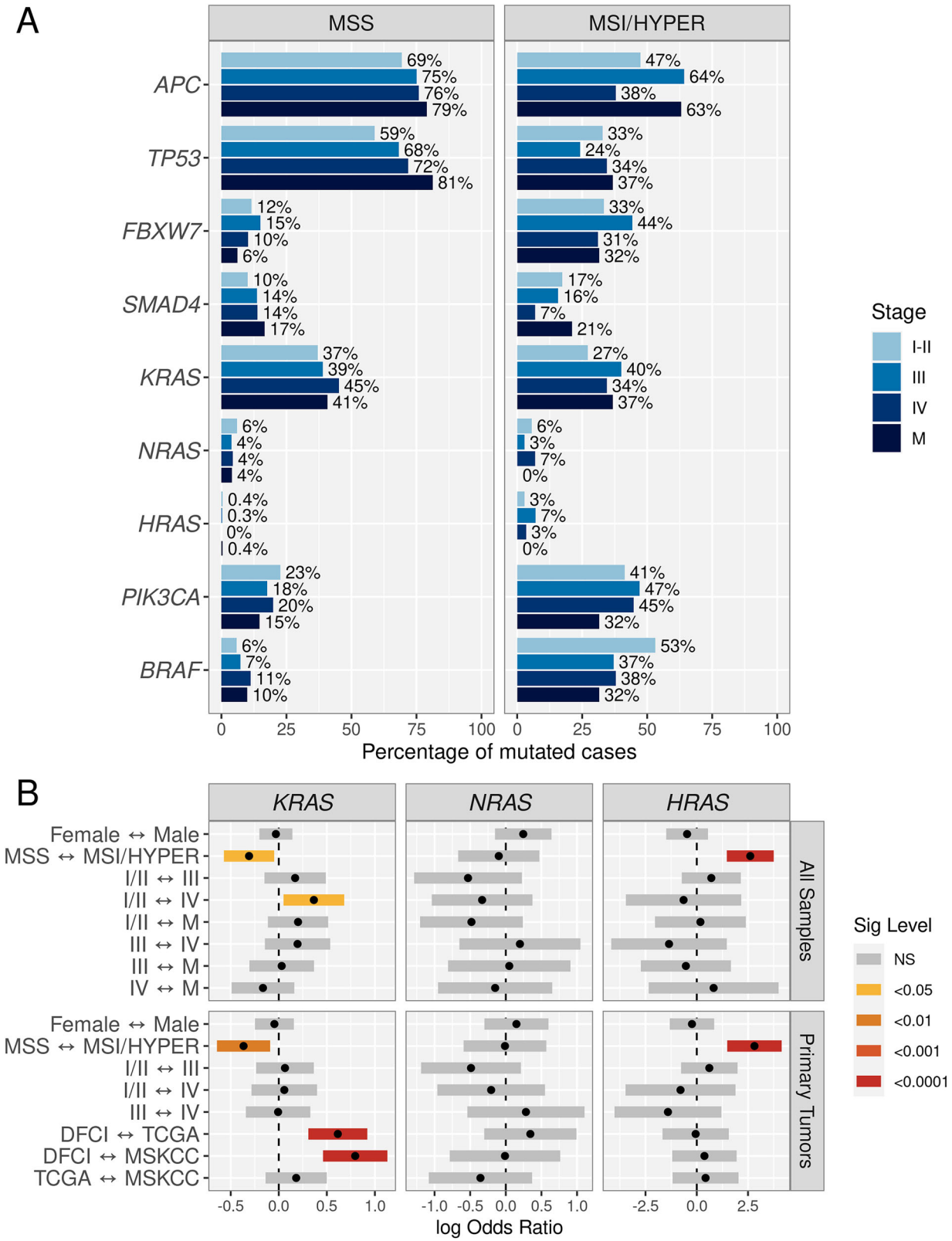

Fig. 1 | Mutational frequency of *RAS* genes and other frequently mutated genes in CRC. A Mutational frequency of the most commonly mutated cancer-related genes in primary CRCs (stage I-II, III, or IV) and metastases of colorectal origin (M). Cases were classified as MSS (left) or MSI/hypermutated (right) based on their MSI status and tumor mutational burden (see "Methods"). **B** Differences in mutational frequency of Ras genes, analyzed by multivariable logistic regression. Dots indicate the log odds ratio (x-axis). The horizontal bars represent the 95% CI of the log odds ratio, colored by their statistical significance corrected using Tukey's HSD method (Sig Level). Values to the left of the vertical dotted line indicate higher mutational frequency in the group listed first in the corresponding comparison (*y*-axis), while values to the right indicate higher mutational frequency in the group listed second. Two multivariable logistic regression analyses are shown: one including all samples and using sample type (primary tumor or metastasis) as a covariate (upper row), and another exclusively comprising primary tumors to allow for the inclusion of cohort as a covariate (lower row).

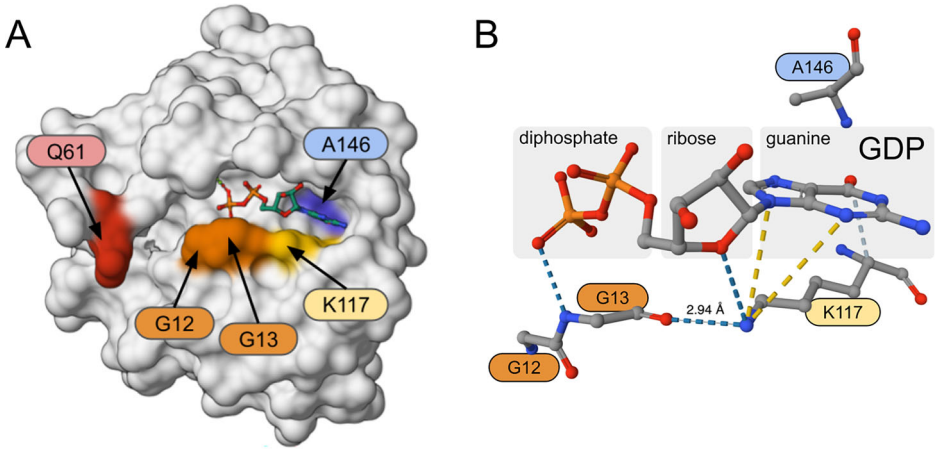

Fig. 2 | Structure of GDP-bound wild-type KRAS. **A** Surface representation of the KRAS protein, highlighting frequently mutated residues. Residues Q61 (red), G12 and G13 (orange), K117 (yellow), and A146 (blue) are labeled and color-coded. The bound GDP molecule is shown in ball-and-stick representation. **B** Close-up view of the GDP binding site in wild-type KRAS. The GDP molecule is subdivided into diphosphate, ribose, and guanine moieties. Atoms are color-coded (carbon in gray, oxygen in red, nitrogen in blue, and phosphorus in orange). Key interactions between KRAS residues (G12, G13, K117, and A146) and GDP are shown as dashed lines: hydrogen bonds (blue), ionic interactions (yellow), and weak hydrogen bonds (gray). The distance between the oxygen of G12 and the nitrogen of K117, forming a hydrogen bond, is 2.94 Å. Structure from reference[66] (ID: 5W22).

primary tumor and one metastasis were analyzed, revealing a high concordance in *KRAS* mutation status between primary and metastatic lesions (17/19, 89%). This observation is consistent with the clonal origin of *KRAS* mutations and in line with previous reports[43]. Only two cases, P-0002463 and P-0012418, showed discrepancies between the mutational status of the primary tumor and the associated metastasis. The primary tumor of patient P-0002463 was *KRAS* wild-type, while the metastasis harbored a G12A mutation. The mutation was detected in only 8.8% (138 out of 1570) of the next-generation sequencing reads interrogating that chromosomal location, suggesting that the mutation was a secondary event acquired after clonal expansion. Conversely, in P-0012418, the *KRAS* G13C mutation was present in the primary tumor but not reported in the metastasis. The mutation was present in only 3.5% of the reads (29 out of 811), suggesting that the *KRAS* mutation was not clonal in the primary tumor and the cells that generated the metastasis were *KRAS* WT, or that the mutant allele was lost during tumor progression.

Mutational profile of KRAS in CRC

The most common *KRAS* mutations (i.e., those at codons G12, G13, Q61, K117, and A146) cluster around the GTP/GDP binding pocket (Fig. 2). Residues G12 and G13 are situated within the P-loop, in close proximity to the di/triphosphate moiety of GDP/GTP, and they are involved in the GTP nucleotide stabilization at the active site. Q61 is located at the N-terminus of the switch-II domain, which plays a pivotal role in conformational changes during the transition between the ON and OFF states of KRAS. K117 is located very close to G13 (< 3 Å) and interacts with the guanine and ribose moieties of GDP/GTP. Finally, A146 resides in a densely packed hydrophobic region near the guanine moiety of the GTP/GDP nucleotide, contributing to the specificity of nucleotide binding[44].

We analyzed in more detail the mutational profile of *KRAS* in the 1,748 primary CRC tumors and 532 metastases. When considering all samples together, MSI/hypermutated CRCs exhibited a lower incidence of *KRAS* G12 mutations than MSS CRCs (11% vs. 27%, OR = 0.33, CI = [0.2–0.5], Q-value = 2.6×10^{-10}) (Fig. 3). In contrast, mutations in codons G13, Q61, K117, and A146 did not exhibit statistically significant differences between MSS and MSI/hypermutated CRCs. As expected given their prominent mutator phenotype, MSI/hypermutated tumors exhibited higher incidence of multiple *KRAS* mutations (OR = 5.3, CI = [1.8–15.5], Q-value = 0.003) and mutations in other codons (OR = 4.2, CI = [1.7–10.4], Q-value = 0.003) (Fig. 3). The analysis revealed that the lower incidence of *KRAS* mutations in the DCFI dataset mainly reflected a lower incidence of *KRAS* G12 mutations, compared to the TCGA and MSKCC datasets, both in the MSS cases (19% vs. 29–31%) and in the MSI/hypermutated cases (2% vs. 15–18%). This difference remained statistically significant in multivariable logistic regression analysis, including patient age, biological sex, tumor stage, and MSI status as possible confounders (OR = 0.5, CI = [0.3–0.7], $p = 2.2 \times 10^{-6}$ DFCI vs. TCGA cohorts, and OR = 0.4, CI = [0.3–0.6], $p = 4 \times 10^{-6}$ DFCI vs. MSKCC cohort).

In line with previous literature[45], mutations in codons 12 and 13 collectively accounted for nearly 82% of all *KRAS* mutations in CRC, with the following incidence order G12D > G12V > G13D > G12C > G12A > G12S (Fig. 4). *KRAS* G12D and G13D exhibited similar incidence in MSS and MSI/hypermutated cases (10.8% vs. 7.8%, OR = 1.4, $p = 0.1$ for G12D, and 7.2% vs. 7.5%, OR = 0.96, $p = 0.8$ for G13D, Fisher's exact tests). In contrast, *KRAS* G12V was the second most frequent mutation in MSS cancers but it was much less common in MSI/hypermutated cancers (8.3% vs. 1.8%, $p = 2.3 \times 10^{-6}$), and *KRAS* G12C mutation represented the fourth most common mutation in MSS cases (3.1%) but was not found in any of the 336 MSI/hypermutated cases ($p = 7.6 \times 10^{-5}$) (Fig. 4). Of note, none of the 19 MSI/hypermutated metastases harbored the very prevalent *KRAS* G12D mutation, despite this mutation being present in 13% (13/97) of the MSI/hypermutated primary tumors of the same study (MSKCC). This difference, however, did not reach statistical significance ($p = 0.12$).

Lower incidence mutations were found at codons 61 (4.5% of all *KRAS* mutations: Q61H > Q61K > Q61R > Q61L), A146 (7.4% of all *KRAS* mutations, A146T > A146V > A146P), and K117 (K117N > K117R). These mutations did not show statistically significant differences between MSS and MSI/hypermutated CRCs, except for *KRAS* Q61K that was more frequent in MSI/hypermutated (2.1%) than in MSS CRCs (0.31%, OR = 6.9, $p = 0.001$).

We found some disparities in the *KRAS* mutational frequencies among studies. Multivariable logistic regression analysis on the primary tumors, including patient age, biological sex, tumor stage, and MSI status as possible confounders, revealed statistically significant differences in the incidence of G12D and G12V among studies, mainly reflecting a lower incidence of these mutations in the DFCI dataset.

Co-mutation analysis

Oncogenic mutations in *KRAS, NRAS, HRAS*, and *BRAF* are generally considered mutually exclusive due to their overlapping downstream effects. Consequently, having oncogenic mutations in multiple genes from the same signaling pathway would not necessarily provide a significant additional growth advantage to cancer cells. Atypical *BRAF* mutations (non-V600E, such as class 2 variants with reduced kinase activity and class 3 variants with impaired or absent kinase activity) frequently co-occur with additional RAS pathway mutations[46]. Nevertheless, *KRAS* mutations can co-occur with mutations in other cancer genes, which can limit the efficacy of KRAS-targeted therapies or, conversely, be exploited in combinatorial therapies to improve patient outcomes.

We analyzed co-mutations of *KRAS, NRAS* and *HRAS* with the rest of the 341 cancer-related genes included in the IMPACT-341 sequencing panel, which represents the minimal gene set analyzed in all samples. To control for the confounding effect of the MSI/hypermutated phenotype on

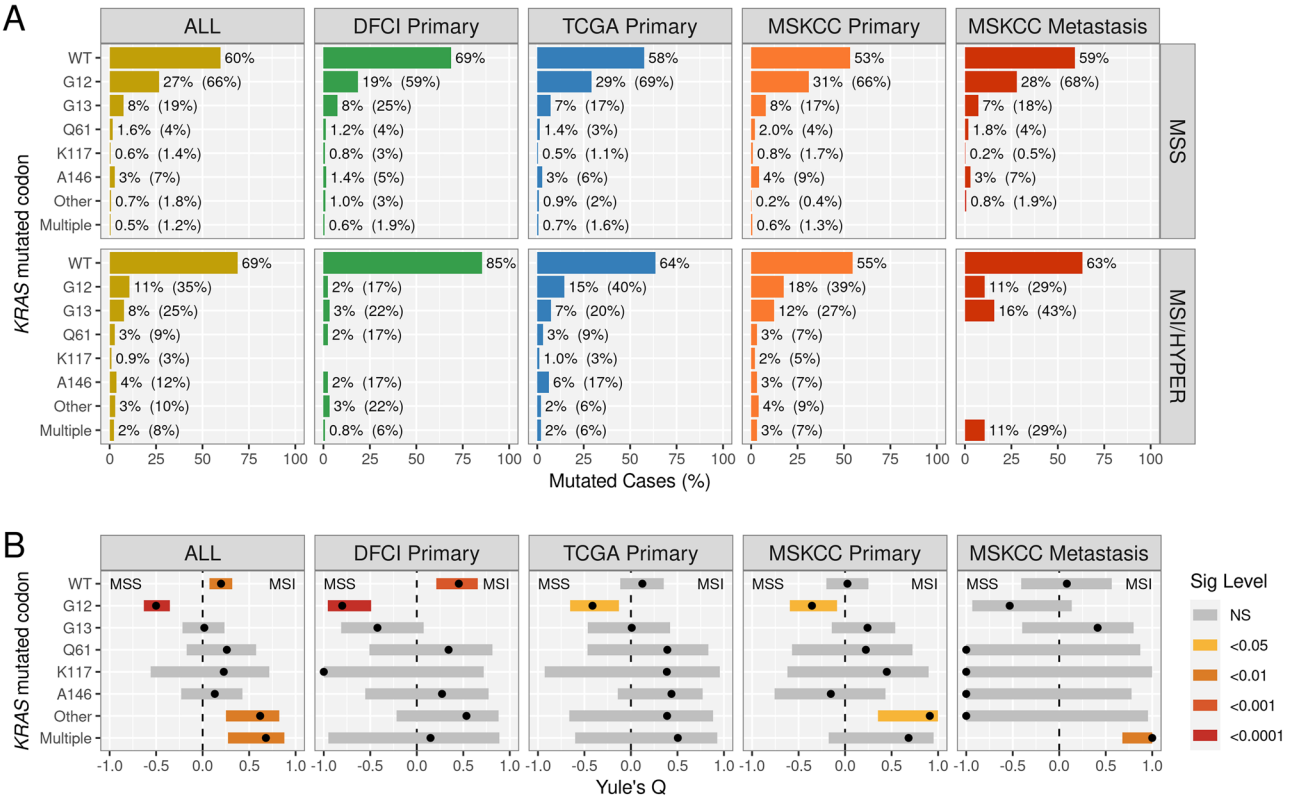

Fig. 3 | *KRAS* codon-specific mutational frequency in CRC. A Frequency of *KRAS* wild-type (WT) and *KRAS* mutant by codon in all samples (ALL) and by cohort. Two percentages are shown for each group: outside parentheses, relative to all samples in the cohort; in parentheses, relative to *KRAS* mutants. **B** Differences in codon-specific *KRAS* mutation frequency between MSS and MSI/hypermutated samples were analyzed using Fisher's tests. To plot associations with extreme odds ratios, Yule's *Q*-values were calculated (see "Methods"). Points to the right of the dotted vertical line (Yule's $Q = 0$) indicate higher frequency in MSI/hypermutated (MSI) tumors, while points to the left indicate higher frequency in MSS tumors. The horizontal bars represent the 95% CI of Yule's *Q*-values, colored by their statistical significance level after correction for multiple-hypothesis testing using the FDR method (Sig Level).

overall mutation frequency—and thus on co-mutation probability—analyses were conducted separately for MSS and MSI/hypermutated primary tumors.

In MSS primary CRCs, *KRAS* mutations were significantly associated with a higher frequency of mutations in *APC, PIK3CA, FBXW7, AMER1*, and *SMAD2*, and with a lower frequency of mutations in *BRAF, NRAS*, and *TP53*. Mutations in *NRAS* were associated with a higher frequency of mutations in *APC*, and with a lower frequency of mutations in *KRAS*. In MSI/hypermutated CRCs, *KRAS* mutations were associated with a higher frequency of mutations in *APC*, and with a lower frequency of mutations in *BRAF* (Fig. 5). For comparison, co-mutation analyses of other frequently mutated genes (i.e., *APC, TP53, FBXW7, SMAD4, PIK3CA*, and *BRAF*) are provided in supplementary Fig. S3.

We identified concomitant *KRAS* and *BRAF* mutations in 1.2% (22/1748) of primary CRCs and 1.5% (8/532) of metastases. Most of these cases harbored atypical *BRAF* mutations (non-V600E, $n = 23$, 77%), and six cases (40%) carried atypical *KRAS* mutations (in codons other than G12, G13, Q61, K117, or A146). In MSS tumors, no concomitant *KRAS* and *BRAF* V600E mutations were observed. Only four tumors, all MSI/hypermutated, showed co-occurrence of *BRAF* V600E with established oncogenic *KRAS* mutations (two G12D, one G12A, and one G13D); notably, both *KRAS* G12D cases also carried atypical *BRAF* mutations alongside V600E, potentially affecting BRAF functionality (supplementary Fig. S4).

KRAS codon-specific co-mutation analysis

We investigated whether tumors harboring different *KRAS* mutations exhibit distinct mutation profiles in other cancer-related genes. Specifically, we assessed whether mutations at the most commonly altered *KRAS* codons (G12, G13, Q61, K117, and A146) were linked to differences in the mutation frequencies of the 340 genes included in the IMPACT-341 panel. In microsatellite-stable (MSS) primary tumors with *KRAS* mutations, we did not observe statistically significant variations in the mutation rates of other genes associated with the *KRAS* mutated codon. In contrast, in MSI/hypermutated primary tumors, we identified 11 genes whose mutation frequencies differed depending on the *KRAS* mutated codon (Fig. 6). Notably, five of these genes—*DDR2, KDR (VEGFR2), EPHA3, ALK*, and *FLT1 (VEGFR1)*—encode transmembrane receptor protein tyrosine kinases that function in cellular signaling upstream of the MAPK pathway (fold enrichment = 5.37, $p = 9 \times 10^{-4}$, FDR *Q*-value = 0.04).

Co-mutations of KRAS and Ras-GAP encoding genes

KRAS G13 mutants exhibit partial sensitivity to NF1-mediated GTP hydrolysis in vitro[47]. Cancer cell lines harboring *KRAS* G13 or A146 mutations have been reported to display a higher *NF1* co-mutation frequency in comparison to those with G12 mutations. Conversely, cancer cell lines with mutations in Q61 showed no *NF1* co-mutations. In a large collection of tumors from different origins, approximately 12% of the *KRAS* G13-mutated samples harbored mutations in *NF1*, whereas only 5.5% of samples with mutations in *KRAS* G12 were found to harbor *NF1* mutations[47].

In our study, *NF1* mutations were significantly more frequent in MSI/hypermutated than in MSS tumors, in both primary tumors (23.4% vs. 2.1%; OR = 12.5, 95% CI: 8–20; $p < 2 \times 10^{-16}$) and metastases (37% vs. 2.3%; OR = 24, 95% CI: 6.7–81; $p = 8.6 \times 10^{-7}$). *NF1* is a very large gene, spanning over 287 kb with a coding sequence of nearly 8.5 kb (99th percentile), and is thus susceptible to acquiring mutations, particularly in tumors with a mutator phenotype. However, the frequency of *NF1* mutations was not higher than that of other genes of comparable length in either MSS or MSI/

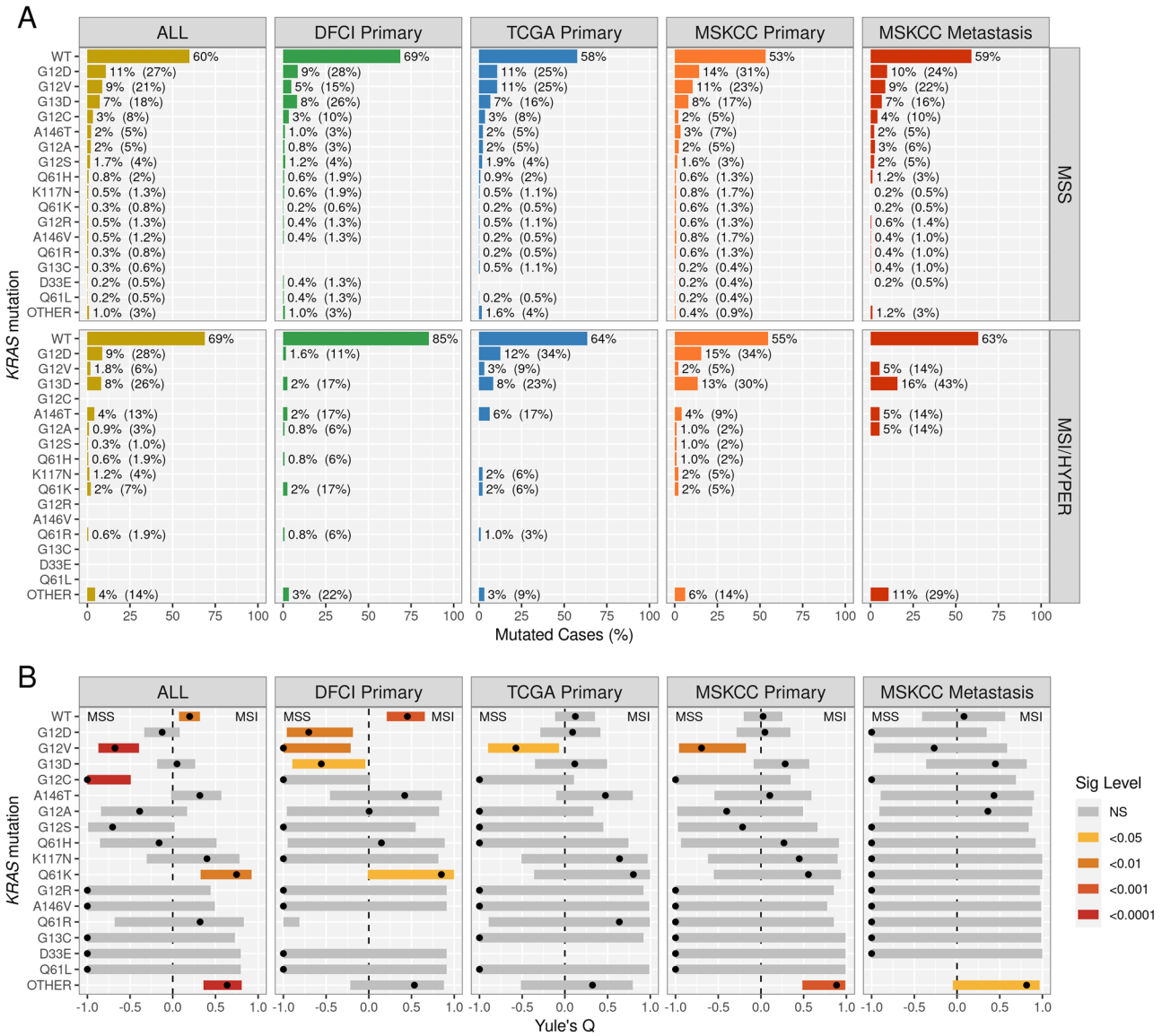

Fig. 4 | *KRAS* mutations in MSS and MSI/hypermutated CRCs. A Mutations in *KRAS* in all samples (ALL, $n = 2280$), and in the different studies, in MSS (upper row, $n = 1945$) and MSI/hypermutated tumors (bottom row, $n = 335$). Mutations are ordered according to their incidence in the whole dataset, including cases with wild-type *KRAS* (WT). Two percentages are shown for each group: outside parentheses, relative to all samples in the cohort; in parentheses, relative to *KRAS* mutants. **B** Differences in codon-specific *KRAS* mutation frequency between MSS and MSI/hypermutated samples were analyzed using Fisher's tests. To facilitate plotting associations with extreme odds ratios, Yule's *Q*-values were calculated (see "Methods"). Points to the right of the dotted vertical line (Yule's $Q = 0$) indicate higher frequency in MSI/hypermutated (MSI) tumors, while points to the left indicate higher frequency in MSS tumors. The horizontal bars represent the 95% CI of Yule's *Q*-values, colored by their statistical significance level after correction for multiple-hypothesis testing using the FDR method (Sig Level).

hypermutated CRCs (supplementary Fig. S5), suggesting the absence of strong positive selection for *NF1* inactivation in CRC.

We found no statistically significant association between *KRAS* G13 mutations and *NF1* mutations in any of the studied CRC cohorts (Fig. 7). In MSS tumors, *NF1* mutations occurred at similarly low frequencies in *KRAS* G12 (0.8%) and G13 (0.9%) mutants, both lower than in *KRAS* wild-type cases (3%). In MSI/hypermutated CRCs, *NF1* mutations were less frequent in *KRAS* G13 mutants (13%) compared to G12 mutants (21%) and wild-type cases (23%), although these differences were not statistically significant. In a multivariable logistic regression model including cohort, sex, age, MSI/hypermutated status, and *KRAS* codon, only MSI/hypermutated status was significantly associated with NF1 mutations ($p < 2 \times 10^{-16}$).

We extended the *KRAS* co-mutational analysis to include *RASA1*, which encodes another important GTPase-activating protein frequently mutated in human cancers. The findings for *RASA1* mutations were similar to those observed for *NF1*. Specifically, we found no evidence of increased mutation frequency in either MSS or MSI/hypermutant CRCs compared to genes of similar size (supplementary Fig. S5), and no association between *RASA1* mutations and the mutational status of *KRAS* (Fig. 7). These observations were further validated on the MSK-CHORD dataset[48], which included over 5000 CRC samples (Supplementary Figs. S6 and S7).

KRAS-targeting compounds

A systematic search of the NCI Thesaurus and PubChem, combining automated searches and manual curation (see "Methods"), retrieved 106 drugs or cellular treatments targeting SHP2/SOS1/KRAS. The list contains 73 inhibitors, 15 TCRs, 14 vaccines, 3 degraders, and 1 antisense. The majority of these compounds directly target KRAS ($n = 89$), while the rest target SOS1 ($n = 5$) or SHP2 ($n = 12$). Most of them targeted a unique *KRAS* mutation (32 for KRAS G12C, 22 for KRAS G12D, 6 for KRAS G12V, and one for KRAS G13N). Nineteen were targeted at multiple *KRAS* mutated isoforms, and 26 were directed at any type of *KRAS* mutation, either because

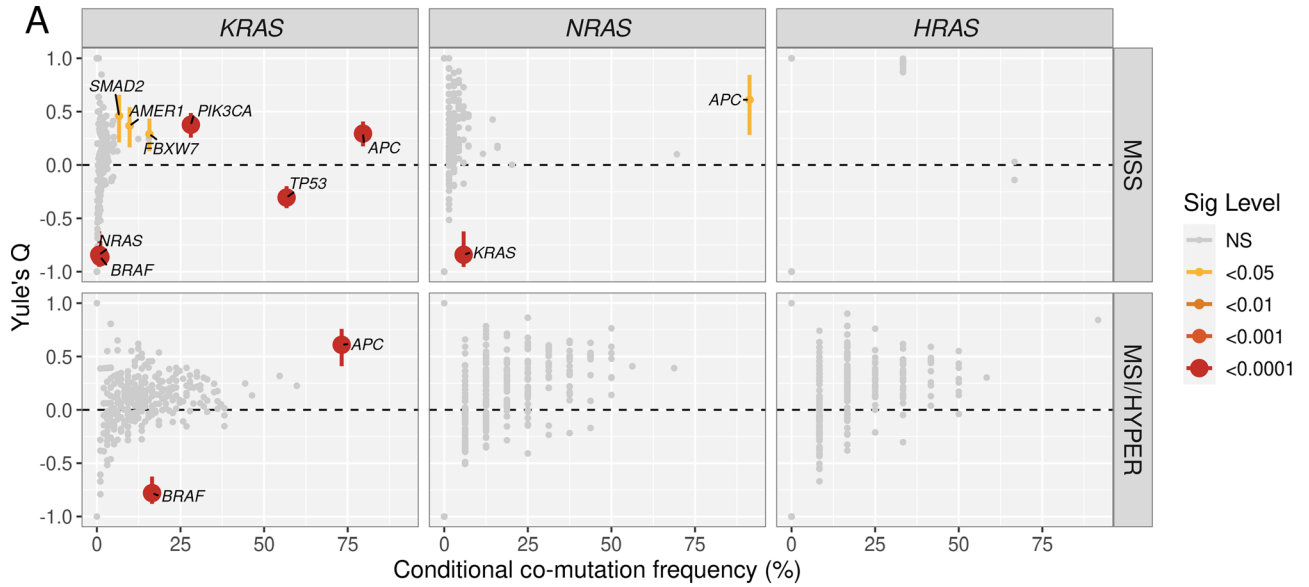

B

GROUP	Gene A	Gene B	OR [CI95%]	FDR	B mutant in A mutant	B mutant in A WT
MSS	KRAS	BRAF	0.07 [0.03-0.17]	7.5e-16	1.0%	12.6%
MSS	KRAS	NRAS	0.09 [0.02-0.23]	1.3e-08	0.7%	7.6%
MSS	KRAS	PIK3CA	2.21 [1.69-2.90]	3.1e-07	28.1%	15.0%
MSS	KRAS	TP53	0.53 [0.42-0.67]	2.2e-06	56.7%	71.1%
MSS	KRAS	APC	1.83 [1.42-2.38]	8.4e-05	79.6%	68.0%
MSS	KRAS	SMAD2	2.70 [1.54-4.85]	1.3e-02	6.6%	2.6%
MSS	KRAS	FBXW7	1.81 [1.30-2.54]	1.5e-02	15.7%	9.3%
MSS	KRAS	AMER1	2.16 [1.40-3.37]	1.5e-02	9.8%	4.8%
MSS	NRAS	KRAS	0.09 [0.02-0.23]	2.6e-08	5.8%	41.7%
MSS	NRAS	APC	4.15 [1.78-11.82]	2.5e-02	91.3%	71.7%
MSI/HYPER	KRAS	BRAF	0.12 [0.06-0.23]	9.3e-12	16.5%	61.6%
MSI/HYPER	KRAS	APC	4.12 [2.39-7.30]	9.1e-06	73.2%	39.7%

Fig. 5 | *KRAS*, *NRAS*, and *HRAS* co-mutation analysis in primary CRCs. A Co-mutation analysis in MSS (upper row) and MSI/hypermutated (lower row) primary CRCs, calculated by Fisher's exact tests. To facilitate plotting associations with extreme odds ratios, Yule's *Q*-values were calculated (*y*-axis). Points above the horizontal dotted line (Yule's $Q = 0$) indicate positive associations (co-mutation), while points below the dashed line indicate negative associations (mutual exclusivity). The vertical lines indicate the 95% CI of Yule's *Q*-values. The colors indicate the statistical significance level, after correction for multiple-hypothesis testing using the FDR method. Genes with an FDR-corrected *p*-value below 0.05 are labeled. The conditional co-mutation frequency (*x*-axis) indicates the proportion of *KRAS*, *NRAS*, or *HRAS* mutant CRCs that also exhibited a mutation in the studied gene. **B** Detailed information of the statistically significant associations found by the co-mutation analysis is shown in panel A. The odds ratio and 95% confidence intervals (OR [CI95%]), and the FDR-corrected *p*-values are shown. In addition, the proportion of cases mutated in gene B in A mutant and A wild-type cases is indicated.

the compound inhibited all KRAS isoforms (including the wild-type) or because it targeted SOS1 or SHP2, inhibiting the GDP to GTP exchange and, consequently, the transition from the inactive to the active form of KRAS. Eighty-five of these compounds have been or are currently under study in clinical trials involving CRC patients (Fig. 8). A detailed list of these compounds, their molecular targets, and associated clinical trials is provided in the supplementary tables file (supplementary_tables.zip).

KRAS-targeted therapies in clinical trials for CRC

A systematic examination of the Clinical Trials Database (https://clinicaltrials.gov), combining automatic search and manual curation, retrieved 156 clinical trials that have evaluated or are currently evaluating the response to at least one of those compounds in patients with CRC (see "Methods"). A chronogram of these trials, indicating the compound tested, the target, the phase, and the current status of these clinical trials, is shown in Fig. 9. In addition, a table with the complete information of these 156 clinical trials is provided as supplementary materials (supplementary_tables.zip). The table includes the data provided by the Clinical Trials Database, the data of the studied compound or treatment (type, target), as well as references from PubMed and PubMed Central citing those clinical trials.

Of the 156 clinical trials, 52 evaluated compounds exclusively targeting KRAS G12C (Fig. 9), despite the very low incidence of this mutation in CRC. This is largely due to the earlier development and regulatory approval of G12C inhibitors, which pioneered the interest in KRAS as a druggable target. These agents demonstrated activity in preclinical CRC models and clinical efficacy in NSCLC, prompting their evaluation in other KRAS G12C-mutant tumors, including CRC.

However, the therapeutic landscape is rapidly evolving beyond G12C-specific strategies. An increasing number of recent and ongoing trials are investigating inhibitors targeting other *KRAS* mutations common in CRC, such as G12D and G12V, as well as broader approaches aimed at pan-KRAS inhibition (Fig. 10). Several trials are also evaluating combination therapies, such as pairing KRAS inhibitors with EGFR, SHP2, or immune checkpoint blockade, to overcome resistance and enhance response rates.

Eighty of these trials are currently recruiting patients, and 11 will recruit patients in the near future, reflecting active clinical interest to expand

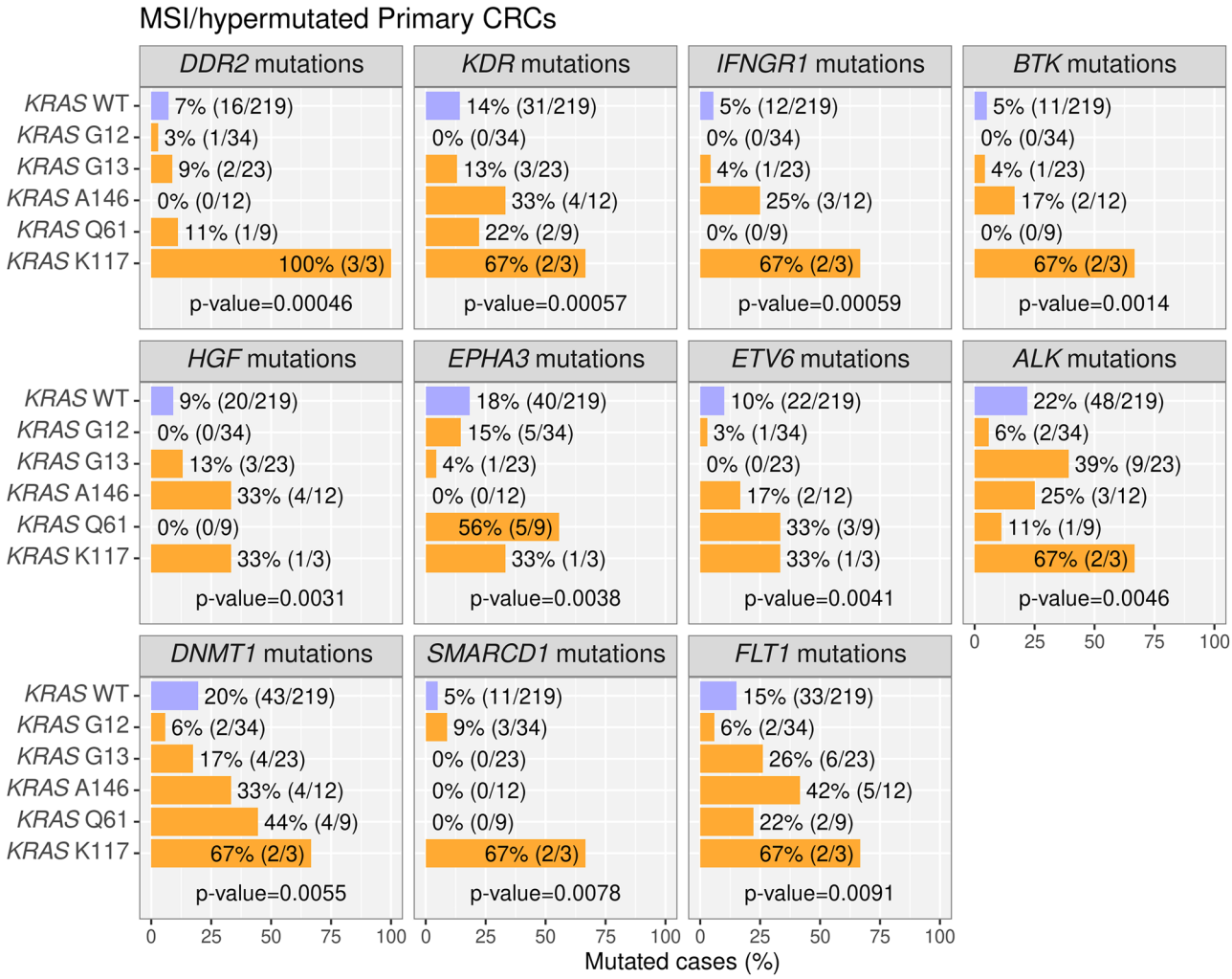

Fig. 6 | Mutated genes associated with codon-specific *KRAS* mutations in MSI/hypermutated primary CRCs. Nominal *p*-values were calculated by Fisher's exact tests on contingency tables, including exclusively the cases with *KRAS* mutations in codons G12, G13, A146, Q61, or K117. Wild-type cases are shown as a reference in the plots, but not used in Fisher's tests. Genes are ordered according to their nominal *p*-value.

the therapeutic options to treat *KRAS*-mutant CRC patients, beyond the narrow subset of *KRAS* G12C–mutant cases.

Discussion

Although *KRAS* is one of the earliest proto-oncogenes identified and the most frequently mutated oncogene in human cancer, it was considered undruggable for nearly 4 decades[20]. This perception has changed in recent years with the development of selective covalent inhibitors targeting KRAS G12C—a mutation that is relatively uncommon in colorectal cancer (CRC) (Fig. 4). More recently, newer drugs targeting more common *KRAS* mutations as well as pan-KRAS drugs that inhibit several or all KRAS isoforms are being tested, potentially broadening the population that could benefit from KRAS-targeted therapies. To ascertain the impact of these new generation KRAS-targeting therapies for CRC patients, it is essential to understand the spectrum of *KRAS* mutations and co-mutations, taking into consideration the genetic heterogeneity of this disease.

We conducted a comprehensive analysis of KRAS mutational frequency using three of the largest publicly available colorectal cancer datasets containing clinical and mutational information. It is important to note that, although patients in these studies were not selected based on their KRAS mutation status, the datasets are not strictly population-based. Notably, the MSKCC study includes a substantially higher proportion of patients diagnosed with Stage IV CRC (~ 60%, Table 1) because its primary aim was to compare metastatic versus non-metastatic CRCs[42]. The frequency of MSI/hypermutated primary tumors was 18.1% (95% CI, 16.3%–20%), consistent with reported frequencies in the CRC patient population (15–20%), with no statistically significant differences observed among the three cohorts (Chi-squared test, $p = 0.24$). As expected, the MSKCC metastatic samples comprise a significantly lower proportion of MSI/hypermutated tumors (3.6%, Table 1), reflecting the lower metastatic potential of MSI CRCs[49]. To reduce potential biases, tumor stage and MSI/hypermutated status were included as covariates in the statistical analyses, or the analyses were performed separately for MSS and MSI/hypermutated tumors.

We provide a detailed overview of the incidence of specific *KRAS* mutations and co-mutations in MSS versus MSI/hypermutated CRCs, and identify substantial differences among the studied datasets that could not be explained by differences in demographics (age, gender) or tumor stage. Differences in *KRAS* mutation prevalence in mCRC patients across populations have been previously described[37]. Higher incidence of *KRAS* mutations in African Americans compared to Caucasian CRC patients has also been reported (OR = 1.56, 95%CI = [1.30-1.87], $p = 0.0001$)[50]. However, the datasets analyzed in our study did not include comprehensive information on patients' genetic ancestry; therefore, we could not determine whether the differences in *KRAS* mutations across datasets were related to variation in genetic ancestry composition.

Most of the *KRAS* codon 12 mutants exhibit a substantial impairment in both intrinsic and GAP-mediated GTP hydrolysis, without altering the nucleotide exchange rate[9]. An exception is the KRAS G12C mutation, where

approximately 75% of the mutant protein is bound to GTP in the steady state, but it still exhibits an intrinsic GTPase activity similar to that of the wild-type KRAS, and much higher than the rest of oncogenic mutations in G12[9,51]. Mutations in RAS proteins can also affect their binding affinity for downstream effectors. For example, the KRAS G12D mutation exhibits approximately a five-fold weaker affinity to RAF1-RBD (Ras-binding domain) compared to wild-type KRAS[9].

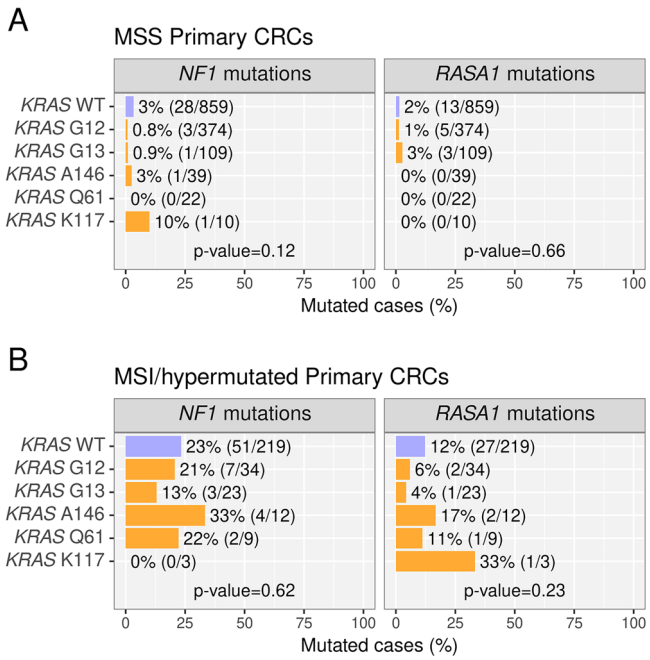

Fig. 7 | Co-mutation analysis of *NF1* and *RASA1* with codon-specific *KRAS* mutations. Frequency of mutations in *NF1* (left) and *RASA1* (right) in MSS (**A**) and MSI/hypermutated (**B**) tumors, classified according to the mutated *KRAS* codon. Nominal p-values were calculated by Fisher's exact tests on contingency tables including the cases with *KRAS* mutations in codons G12, G13, A146, Q61, or K117. Wild-type cases are shown as reference, but not used in the Fisher's tests. No statistically significant associations were found between *NF1* or *RASA1* mutations and the mutated *KRAS* codon.

Previous studies have suggested that *KRAS* mutations at codon 12 display a greater oncogenic potential by impairing apoptosis and enhancing contact-independent growth when compared to mutations at codon 13[52,53]. Both in vitro and in vivo experiments have provided evidence of a higher transforming capacity of mutations at codon 12 compared to codon 13[52]. In a retrospective study focusing on advanced or recurrent CRC, it was observed that patients with mutations at codon 12 displayed worse overall survival compared to patients with wild-type *KRAS*, whereas mutations at codon 13 did not exhibit a statistically significant impact on survival[54]. Further examination in patients with advanced and recurrent CRC revealed that among the five most common codon 12 mutations, G12D and G12V were independently associated with a poorer overall survival after diagnosis[54]. However, more recent studies did not observe a prognostic difference between KRAS G12D and other KRAS mutants[55,56]. Taken together, these findings indicate that the prognostic significance of *KRAS* G12D remains uncertain and may be context dependent, varying with patient population, tumor stage, and co-occurring molecular alterations.

Our analysis revealed significant differences in the frequency of *KRAS* G12 mutations in the DFCI cohort that were not explained by demographic (biological sex or age) or pathological (tumor stage and MSI status) differences with the other two studied cohorts (Figs. 1 and 3).

Albeit *KRAS* mutations are generally considered to be associated with MSS tumors, our analysis indicated that this applies particularly to G12 mutations, as we found no significant differences in the frequency of mutations in other codons (G13, Q61, K117 and A146) between MSS vs. MSI/hypermutated tumors (Fig. 3). Moreover, a more detailed analysis revealed that the most frequent *KRAS* mutation, i.e., G12D, exhibited a similar incidence in MSS and MSI/hypermutated primary CRCs in two of the datasets (TCGA and MSKCC) (Fig. 4). In contrast, G12V was found at much lower frequency, and G12C mutation was never found, in MSI/hypermutated cancers despite their mutator phenotype, highlighting that the oncogenic potential of these two mutations might be influenced by the genetic background of the cell.

Mutations in codon 13 of *KRAS* exhibit distinctive characteristics. Specifically, codon 13 mutants impact hydrolysis and significantly increase intrinsic nucleotide exchange by approximately 10-fold[9]. Notably, it was reported that the tumor suppressor *NF1* is commonly co-mutated in KRAS G13-mutated cells but rarely mutated in cancers with *KRAS* codon 12 or 61 mutations[47]. Interestingly, NF1 GAP protein is inactive against KRAS G12 and Q61-mutated KRAS; however, it stimulates GTP hydrolysis when bound to KRAS G13D. The results suggested that *KRAS* G13D mutant cells

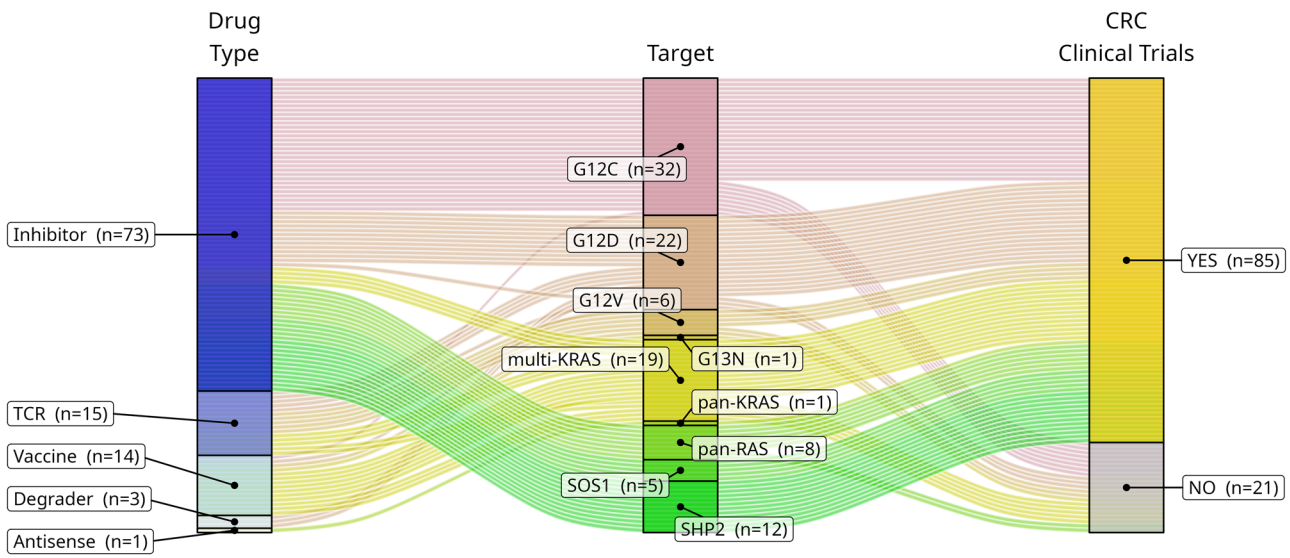

Fig. 8 | Drugs targeting KRAS, SOS1 or SHP2. Diagram of the 106 compounds identified in this study. Every line represents a compound, and connects their type (left column), their target (middle column) and whether they have reached clinical trials on CRC patients (right column). Lines are colored according to the compounds' targets.

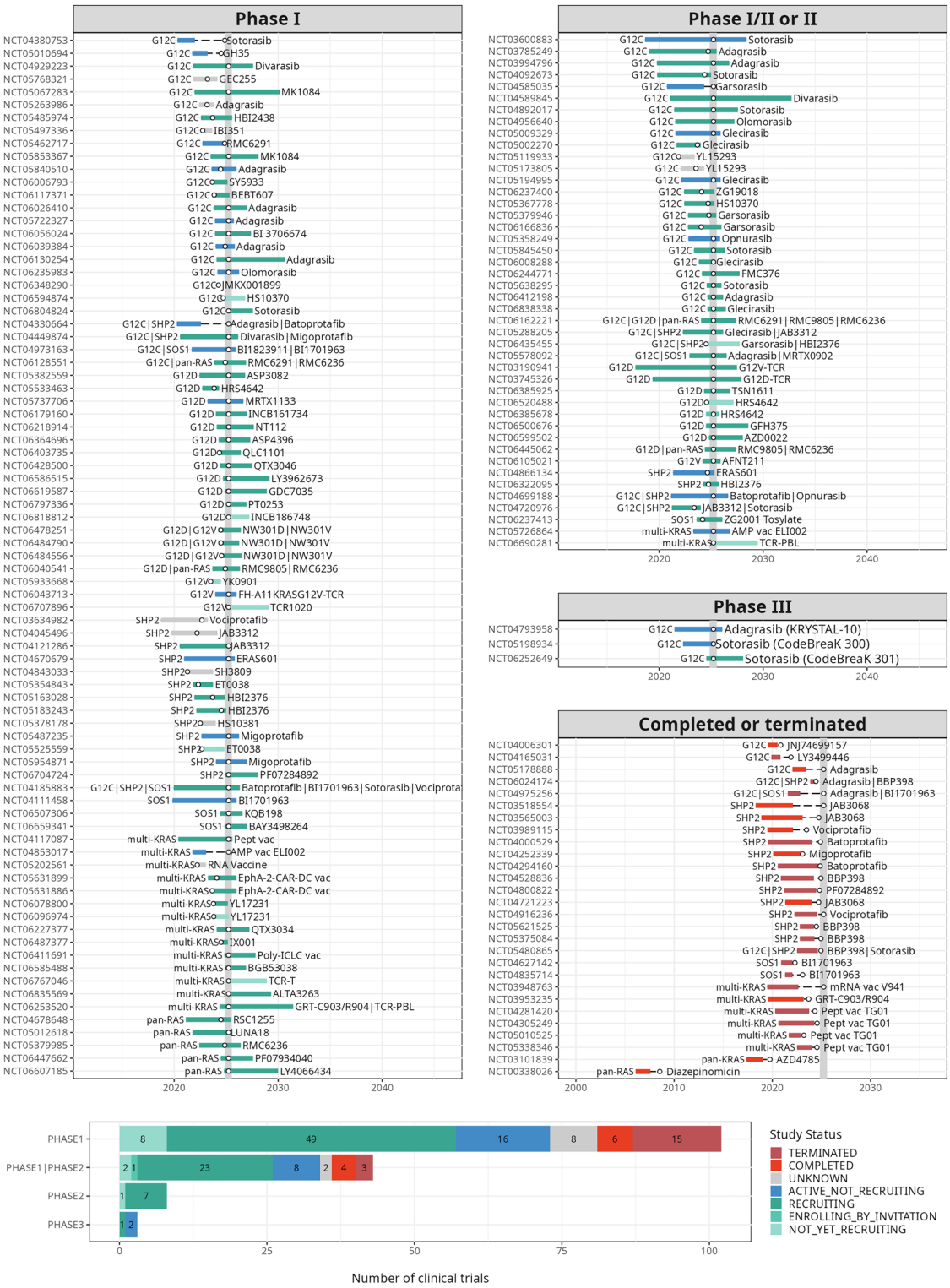

Fig. 9 | Clinical trials studying KRAS-targeted therapies in CRC patients. Chronogram of clinical trials that include at least one of the 106 compounds shown in Fig. 8, evaluating their response in patients with solid malignancies, including CRC. The horizontal segments represent the planned start and finalization dates of the clinical trials. On the left side of each bar, the target *KRAS* mutation or KRAS-related protein is indicated. On the right side, the KRAS-related drug or drugs are indicated. Clinical trials have been organized in different panels by study phase, and colored based on the study status. The white dots indicate the latest information update. The vertical gray bar indicates the current date. Data were obtained from the Clinical Trials database (https://clinicaltrials.gov), retrieved as detailed in "Methods".

can also respond to EGFR inhibitors in an NF1-dependent manner. The clinical observation that *KRAS* G13D CRC may respond to EGFR inhibition could be explained by the increased sensitivity to NF1-stimulated GTP hydrolysis. In the presence of an active and functional NF1, *KRAS* G13D cancer cells may have reduced KRAS GTP levels and be partially dependent on upstream signaling through EGFR or other receptor tyrosine kinases[47]. In our analysis, we did not observe significant enrichment of *NF1* or *RASA1* mutations in association with any specific *KRAS* codons, suggesting that NF1 inactivation is not a recurrent mechanism to potentiate KRAS-driven oncogenesis in CRC. Moreover, mutation frequencies of both *NF1* and

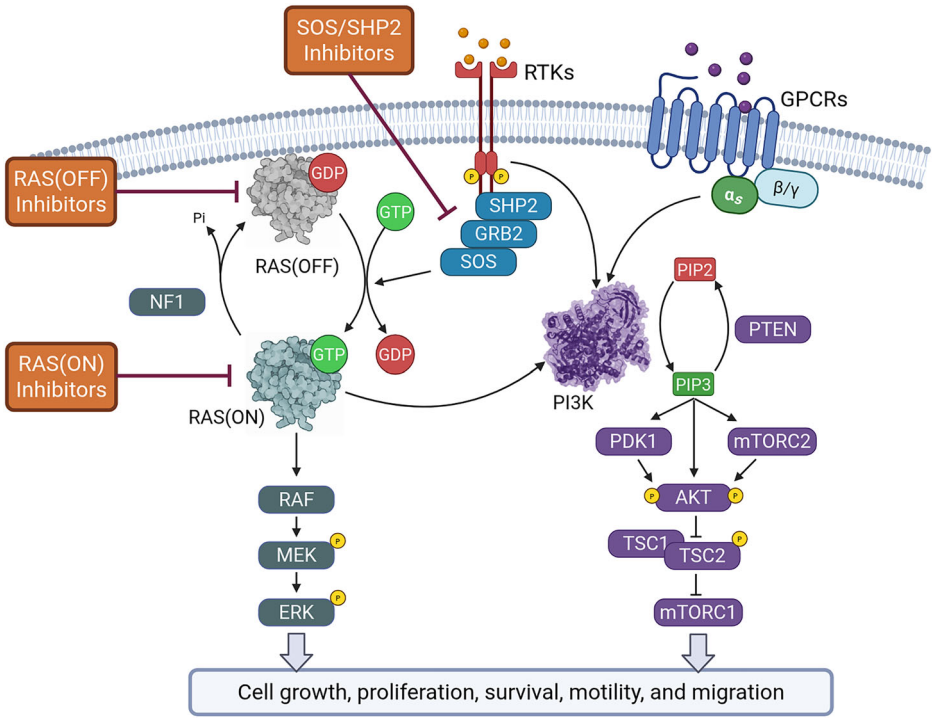

Fig. 10 | Ras/MAPK and PI3K/AKT/mTOR signaling pathways. Upon ligand binding (represented as yellow spheres outside the cell membrane), receptor tyrosine kinases (RTKs) recruit adaptor proteins (SHP2, GRB2, and SOS) that promote the exchange of GDP for GTP on KRAS, leading to its activation (KRAS-GTP). Activated KRAS stimulates downstream signaling through RAF, MEK, and ERK, promoting cell growth, proliferation, survival, motility, and migration. Both RTKs and G protein-coupled receptors (GPCRs) can activate PI3K via Gβγ subunits, catalyzing the conversion of PIP2 to PIP3. PIP3 facilitates the membrane recruitment and activation of AKT by PDK1 and mTORC2. Activated AKT regulates downstream effectors, including the TSC1/2 complex and mTORC1, to control cellular growth and survival. Negative regulation is mediated by RAS-GAPs (e.g., NF1) and PTEN, a lipid phosphatase that converts PIP3 back to PIP2. Targets of the compounds discussed in this study are indicated in orange boxes. As of June 1, 2025, only sotorasib and adagrasib, both targeting RAS(OFF) G12C, have been approved by the FDA for the treatment of CRC. Additional therapeutic agents targeting upstream of RAS, not discussed in this work (e.g., cetuximab, panitumumab, bevacizumab, ramucirumab, fruquintinib, regorafenib, tucatinib, and ziv-aflibercept), have also received FDA approval for CRC treatment.

RASA1 were similar to those of other genes of similar length in both MSS and MSI/hypermutated tumors, suggesting that mutations in these genes are not under strong selection for tumorigenesis or tumor progression. The higher *NF1* mutation frequency in MSI/hypermutated tumors likely reflects the underlying hypermutator phenotype rather than functional selection.

Glutamine-61 (Q61) is situated in the switch-II region of the GTP hydrolysis domain of KRAS (Fig. 2). Mutations in this residue impair both intrinsic and GAP-mediated GTP hydrolysis. These mutations also accelerate the rate of GDP-GTP exchange, leading to an accumulation of the mutant protein in the GTP-bound state[9]. In particular, mutations in Q61H and Q61L have been shown to result in a substantial reduction, approximately 40- to 80-fold, in the intrinsic hydrolysis rate when compared to WT *KRAS*. Furthermore, these mutations exhibited a significant decrease in the rate of GAP-stimulated hydrolysis compared with WT KRAS[9]. However, the GAP-stimulated rate for Q61L was approximately 15-fold higher than its intrinsic rate, suggesting that a portion of the GAP-dependent catalytic mechanism is still partly functional in the Q61L mutant. Consistent with these observations, similar to G12 and A146 mutants, CRC tumors harboring Q61 mutations exhibit resistance to anti-EGFR therapy, suggesting that these mutations impair the response to GAP-stimulated hydrolysis in vivo[57].

Mutations at codon 117 of *KRAS*, although less frequent than those in codons 12, 13, or 61, represent a distinct class of activating alterations. The K117N mutation promotes constitutive activation of KRAS through enhanced nucleotide exchange and reduced GTP hydrolysis, although to a lesser extent than G12 or Q61 mutants[58]. Biochemically, K117 mutations exhibit moderate impairment in GAP-stimulated GTP hydrolysis and increased binding to effectors such as RAF, supporting their oncogenic potential. Functionally, they confer growth factor-independent signaling, although often with lower transforming activity than classical G12 mutations[9]. Clinically, the predictive value of K117 mutations for anti-EGFR therapy remains ambiguous. Some retrospective analyses have included K117 among non-canonical *RAS* mutations associated with resistance to EGFR blockade, though the evidence is limited by the low incidence of this mutation[59]. The relatively low frequency and intermediate biochemical phenotype of K117 mutations highlight the need for further mechanistic studies and clinical stratification.

Mutations at codon A146 of *KRAS* exhibit distinct characteristics. A study conducted by Poulin et al. revealed that the *KRAS* A146T mutation displayed an in vitro intrinsic GTP hydrolysis activity similar to that of *KRAS* G12D but considerably lower than that of *KRAS* WT. However, GAP-mediated GTP hydrolysis was significantly impaired for *KRAS* G12D, but only mildly impaired for *KRAS* A146T. Additionally, mutations in *KRAS* A146 led to an increase in GEF-mediated nucleotide exchange without affecting GAP activity[60]. Data regarding the effect of anti-EGFR treatment in patients with CRC harboring a *KRAS* A146 mutation are conflicting. Some studies have described a more favorable clinical outcome in patients with CRC carrying a *KRAS* A146-mutated tumor when subjected to anti-EGFR treatment, in comparison to patients with tumors carrying other *KRAS* mutations[61]. Conversely, other studies have shown that tumors with a *KRAS* A146 mutation are associated with resistance to anti-EGFR therapy[59,62].

As of June 2025, only adagrasib and sotorasib have been approved by the FDA to treat CRC patients. Adagrasib (Krazati) was FDA-approved for *KRAS* G12C-mutated locally advanced or metastatic CRC on June 21, 2024. The approval was granted for use in combination with cetuximab (Erbitux) in patients who had previously been treated with fluoropyrimidine-, oxaliplatin-, and irinotecan-based chemotherapy[63]. Sotorasib (Lumakras) in combination with panitumumab (Vectibix) was approved by the FDA for CRC on January 16, 2025. This approval was specifically for adult patients with *KRAS* G12C-mutated metastatic CRC, who have received prior fluoropyrimidine-, oxaliplatin-, and irinotecan-based chemotherapy[64]. The European Medicines Agency (EMA) has not yet approved either sotorasib or adagrasib for CRC treatment, though these agents may be accessible via clinical trials or compassionate use. Despite their approval, these two inhibitors exclusively target the rare *KRAS* G12C mutation, which occurs in approximately 3% of the MSS CRC cases and is not found in MSI/hypermutated cases (Fig. 4), thereby limiting its applicability for the vast majority of CRC patients.

Of the 156 clinical trials, 52 evaluated compounds exclusively targeting KRAS G12C (Fig. 9), despite the very low incidence of this mutation in CRC. This is mainly due to the earlier development and regulatory approval of G12C inhibitors, which pioneered the interest in KRAS as a druggable target. These agents demonstrated activity in preclinical CRC models and

clinical efficacy in NSCLC, prompting their evaluation in other *KRAS* G12C-mutant tumors, including CRC.

Despite the current limitations of G12C inhibitors, the therapeutic landscape for *KRAS*-mutant colorectal cancer is rapidly evolving. A large and growing number of clinical trials are now underway (Fig. 9), investigating new agents designed to target other, more prevalent *KRAS* mutations such as G12D, G12V, and G13D. These efforts reflect a major shift in drug development, moving beyond the narrow focus on G12C to address the broader spectrum of *KRAS* alterations that account for the majority of *KRAS*-mutant CRC cases. In particular, the emergence of pan-RAS and RAS(ON) inhibitors represents a significant breakthrough. These agents are designed to inhibit multiple KRAS mutant isoforms or to target KRAS in its active, GTP-bound state, thereby overcoming the mutation-specific limitations of earlier compounds. Several of these novel inhibitors are already in phase 1 and 2 clinical trials (Fig. 9), and early results suggest that they may offer meaningful clinical benefits for a much larger proportion of CRC patients.

Several trials are also evaluating combination therapies, such as pairing KRAS inhibitors with EGFR, SHP2, or immune checkpoint blockade, to overcome resistance and enhance response rates. Additionally, immunotherapeutic strategies targeting mutant *KRAS* are gaining momentum. Approaches such as peptide vaccines, mRNA vaccines, and T-cell receptor (TCR)-engineered therapies are being actively investigated in clinical settings. These therapies aim to harness the immune system to specifically recognize and eliminate *KRAS*-mutant tumor cells, offering new hope for durable responses.

Taken together, these ongoing efforts may mark a new era in the management of *KRAS*-mutant CRC. The diversity and scale of current clinical trials reflect a strong commitment and interest in overcoming the historical challenges of targeting KRAS. As these new therapies advance through clinical development, there is increasing optimism that effective, mutation-inclusive treatment options will soon become available for a much broader population of CRC patients.

Our study provides a comprehensive and updated overview of *KRAS* mutations and therapeutic strategies in colorectal cancer, integrating large publicly available datasets with curated information from multiple databases and clinical trial registries. A major strength is the systematic approach to cross-reference compounds, clinical trials, and mutational frequencies, with careful stratification of MSS versus MSI cases, which improves accuracy and clinical relevance. Our work also highlights clinically meaningful co-mutation patterns and contextualizes ongoing therapeutic efforts, offering value as both a resource and a reference for the field. Taken together, our integrative analysis highlights the importance of codon- and context-specific characterization of *KRAS* mutations to guide precision oncology in CRC. However, we acknowledge several limitations. First, the study relies on publicly available datasets, which, although large and valid for this type of analysis, are not population-based and therefore subject to selection bias; mutation frequencies may not fully reflect those observed in unselected, population-derived cohorts. Second, database annotations may be incomplete or inconsistent, and despite extensive cross-referencing, some compounds or trials may have been missed due to indexing practices or variable reporting standards. Finally, KRAS-targeting therapies is a rapidly evolving field, and additional compounds and clinical trials not included in our study are likely to emerge in the near future.

In summary, our study confirms established knowledge and identifies novel insights into *KRAS* mutations in CRC. *KRAS* mutations are highly prevalent in CRC, most commonly affecting codons 12 and 13, and less frequently in codons 61, 117, and 146. Their high concordance between primary and metastatic lesions reflects an early, clonal origin. Our analysis shows that mutation distribution drastically differs by microsatellite instability status. MSS tumors frequently harbor *KRAS–PIK3CA* co-mutations. In MSS primary CRCs, *KRAS* mutations frequently co-occur with *PIK3CA* mutations. This co-mutation pattern might be clinically significant, as targeting KRAS alone may not be sufficient to inhibit tumor growth. In contrast to previous reports, we found no association between *KRAS* G13 mutations and *NF1* mutations; *NF1* alterations were instead linked to MSI/hypermutated tumors at rates similar to other large genes. Therapeutically, current FDA-approved inhibitors target only *KRAS* G12C, a rare variant in MSS CRC and virtually absent in MSI CRC. However, the treatment landscape is rapidly expanding to include inhibitors of more common *KRAS* alleles (e.g., G12D, G12V, G13D), pan-RAS and RAS(ON) agents, and immunotherapies such as vaccines and TCR-based therapies.

Methods

Colorectal cancer datasets

Mutational and clinical data were obtained from two main sources: the Catalog Of Somatic Mutations in Cancer (COSMIC)[38] and the colorectal cancer cohorts accessible from cBioportal[65]. Three cohorts were accessed: DFCI (619 primary CRCs)[40], TCGA Pancancer (594 primary CRC samples)[41], and MSKCC (601 primary CRC samples and 533 metastases)[42]. During the preparation of this manuscript, a larger dataset from the MSK-CHORD study became available[48]. This pan-cancer dataset included 5,543 CRC samples from the MSKCC, some of which overlapped with those used in our analysis. However, the clinical information associated with the dataset lacked patients' age at diagnosis (instead providing their current age, which differed from previously published overlapping datasets), and the stage information was less detailed than that of the datasets used in our analysis. These limitations made it difficult to integrate the MSK-CHORD data with the other datasets. More importantly, the significantly larger number of samples in the MSK-CHORD dataset compared to the DFCI and TCGA datasets would introduce substantial bias into the analyses. Therefore, we decided not to include the MSK-CHORD dataset in this study. Nevertheless, we used this dataset to validate observations such as co-mutation associations and the lack of association between *KRAS* G13 and *NF1* mutations.

Sixty-six cases from the TCGA cohort and 1 case from the MSKCC cohort with no mutational information were excluded from the subsequent analyses. The data did not include biological sex information from two patients, i.e., TCGA-M5-AAT5 and TCGA-M5-AATA. The biological sex of these patients (female and male, respectively) was inferred from the methylation profile of chromosome X, obtained from the GDC Data Portal (https://portal.gdc.cancer.gov/). Fourteen TCGA cases and 56 DFCI cases did not include tumor stage information. In the TCGA cases, tumor stage could be determined from the TNM information upon individual inspection of their pathology reports accessed from the GDC Data Portal. For the 56 DFCI cases, pathology reports were not publicly available, and thus, the tumor stage could not be determined. The combined dataset contained 2287 CRCs. Cases were classified as MSS or MSI based on the annotated MSI status: DFCI (438 MSS, 91 MSI-high, 90 non-determined) and MSKCC (701 MSS, 105 MSI, and 328 non-determined or inconclusive) cases. TCGA cases with an MSI MANTIS score over 0.4 were classified as MSI. Hypermutated tumors were identified based on their non-synonymous tumor mutation burden (TMB). DFCI and TCGA samples with a TMB over 14 mutations per Mb were considered hypermutated, while for the MSKCC samples, a TMB threshold of 25 mutations per Mb was applied, as previously reported[41]. The different thresholds were justified by the difference in TMB among the cohorts (Supplementary Fig. S8), resulting from the use of different sequencing strategies. TCGA and DFCI datasets were analyzed by whole-exome sequencing (WES), whereas MSKCC samples were sequenced using targeted panels enriched in cancer-related genes (IMPACT-341 for 214 samples, IMPACT-410 for 910 samples, and IMPACT-468 for nine samples). For all analyses, cases were classified into MSS and MSI/hypermutated, following the classification proposed by the TCGA[4].

Co-mutation analysis

Mutational data were obtained from cBioportal[65]. The study was focused on the 341 genes analyzed in all the samples (those included in the IMPACT-341 sequencing panel) (supplementary_tables.zip). For each gene pair (A and B), the conditional co-mutation frequency (CCMF) was calculated as the percentage of samples with mutations in gene A that also had mutations in gene B (CCMF = 100 x (N_{AB}/N_A), where N_{AB} is the number of samples with mutations in both genes A and B, and N_A is the number of samples

mutated in gene A). The statistical analysis of co-mutations was conducted using Fisher's exact test on contingency tables for univariate analyses, or by logistic regression followed by Tukey's honest significant differences post-hoc (Tukey's HSD) for multivariable analyses. To graphically represent odds ratios (OR) with extreme values (such as when they equal zero or infinity), we employed Yule's coefficient of association, which is a normalized transformation of the odds ratio ($Q = (OR - 1)/(OR + 1)$). A Q-value of +1 indicates perfect co-occurrence, −1 indicates perfect mutual exclusivity, and 0 indicates no association. Unlike ORs, Yule's Q compresses large effect sizes and avoids singularities, providing more interpretable and visually stable comparisons across genes with widely varying mutation frequencies.

KRAS 3D rendering

The structure of GDP-bound wild-type KRAS was obtained from ref. 66 (ID: 5W22), available at the PDB databank (http://www.rcsb.org)[67] and rendered using Mol*[68].

Statistical analyses

Statistical analyses were performed using the R language for statistical computing[69]. Departure from normality was determined by the Shapiro-Wilk test. Normally distributed variables were analyzed with parametric tests (i.e., *t*-test, ANOVA). Non-normally distributed variables were analyzed using non-parametric tests (Wilcoxon–Mann–Whitney test, Kruskal–Wallis test). Differences in proportions were analyzed by Fisher's exact test on contingency tables for univariate analyses or by logistic regression for multivariable analyses. Pairwise comparisons between the levels of the categorical variables were assessed using the *pairs* function from the emmeans package, which applies pairwise t-tests on the marginal means, adjusted for multiple comparisons using Tukey's method. Gene set enrichment analysis was performed using PANTHER Overrepresentation Test (https://pantherdb.org/tools/). Nominal p-values below 2×10^{-16} were summarized as p-value $< 2 \times 10^{-16}$. When required, correction for multiple-hypothesis testing was performed using the false discovery rate method (FDR). FDR-corrected p-values (named Q-values) below 0.05 were considered statistically significant.

Compilation of KRAS-targeting compounds, clinical trials, and bibliography review

Updated information about Ras-targeting therapies in CRC was obtained by consulting PubMed (https://pubmed.ncbi.nlm.nih.gov/), PubChem (https://pubchem.ncbi.nlm.nih.gov/)[70], the NCI Thesaurus (https://evsexplore.semantics.cancer.gov/), the ClinicalTrials database (https://clinicaltrials.gov/) and the FDA Oncology (Cancer)/Hematologic Malignancies Approval Notifications website (https://www.fda.gov/drugs/resources-information-approved-drugs/oncology-cancer-hematologic-malignancies-approval-notifications), as of 25th of March of 2025.

From the NCI thesaurus database, we retrieved 66 Ras-targeting compounds (47 inhibitors, 11 vaccines, 6 TCRs, and 2 degraders), 12 SHP2-targeting compounds, and 4 SOS1-targeting compounds. To reduce redundancy, the salt forms of some drugs (e.g., divarasib adipate, rigosertib sodium, sorafenib tosylate, dabrafenib mesylate, lifirafenib maleate, and regorafenib anhydrous) were not considered. Of note, the NCI thesaurus database listed the drugs Paluratide and Ras Inhibitor LUNA18 under two different codes (C206963 and C185876, respectively), when they are the same compound (CID 166509683). Twenty-four therapeutic compounds targeting KRAS, SOS1, or SHP2 that were not indexed in the NCI thesaurus database were found in the clinical trials database and manually added, increasing the number of KRAS/SOS1/SHP2 targeting compounds to 106 (supplementary_tables.zip). We crossed this information with the clinical trials that indicated colorectal, colon, rectal, CRC, or solid tumors in the Conditions field, INTERVENTIONAL in Study Type, and TREATMENT in Primary Purpose, retrieving 153 studies in which at least one of the 106 selected drugs had been or is being tested. We noticed that three important studies, i.e., NCT06385925, NCT04330664, and NCT03785249, were not retrieved using this strategy because they did not specifically indicate colorectal or solid tumors in the Conditions field. These studies were manually added to the list, yielding a total number of 156 clinical trials (supplementary_tables.zip). For 11 clinical trials without information in the Completion Date field, we used the Date of the Last Update Posted. Scientific articles referencing these clinical trials were identified in PubMed (searching in All Fields) and PMC (searching in Title, Abstract or Body-Key Terms).

Ethics approval

Not applicable.

Data availability

Processed datasets are provided in supplementary_tables.zip. Raw data and processing scripts are available upon request to Sergio Alonso (salonsou@igtp.cat).

Code availability

Processed datasets are provided in supplementary_tables.zip. Raw data and processing scripts are available upon request to Sergio Alonso (salonsou@igtp.cat).

Received: 7 July 2025; Accepted: 14 October 2025;
Published online: 26 November 2025

References

1. Filho, A. M. et al. The GLOBOCAN 2022 cancer estimates: data sources, methods, and a snapshot of the cancer burden worldwide. *Int. J. Cancer* **156**, 1336–1346 (2025).
2. Kinzler, K. W. & Vogelstein, B. Lessons from hereditary colorectal cancer. *Cell* **87**, 159–170 (1996).
3. Perucho, M. Cancer of the microsatellite mutator phenotype. *Biol. Chem.* **377**, 675–684 (1996).
4. Cancer Genome Atlas Network. Comprehensive molecular characterization of human colon and rectal cancer. *Nature* **487**, 330–337 (2012).
5. Guinney, J. et al. The consensus molecular subtypes of colorectal cancer. *Nat. Med.* **21**, 1350–1356 (2015).
6. Simanshu, D. K., Nissley, D. V. & McCormick, F. RAS proteins and their regulators in human disease. *Cell* **170**, 17–33 (2017).
7. Scheffzek, K. et al. The Ras-RasGAP complex: structural basis for GTPase activation and its loss in oncogenic Ras mutants. *Science* **277**, 333–338 (1997).
8. Kandoth, C. et al. Mutational landscape and significance across 12 major cancer types. *Nature* **502**, 333–339 (2013).
9. Hunter, J. C. et al. Biochemical and structural analysis of common cancer-associated KRAS mutations. *Mol. Cancer Res.* **13**, 1325–1335 (2015).
10. Prior, I. A., Lewis, P. D. & Mattos, C. A comprehensive survey of Ras mutations in cancer. *Cancer Res.* **72**, 2457–2467 (2012).
11. Varshavi, D. et al. Metabolic characterization of colorectal cancer cells harbouring different KRAS mutations in codon 12, 13, 61 and 146 using human SW48 isogenic cell lines. *Metabolomics* **16**, 51 (2020).
12. Vanhaesebroeck, B., Perry, M. W. D., Brown, J. R., André, F. & Okkenhaug, K. PI3K inhibitors are finally coming of age. *Nat. Rev. Drug Discov.* **20**, 741–769 (2021).
13. Roberts, P. J. & Der, C. J. Targeting the Raf-MEK-ERK mitogen-activated protein kinase cascade for the treatment of cancer. *Oncogene* **26**, 3291–3310 (2007).
14. Canon, J. et al. The clinical KRAS(G12C) inhibitor AMG 510 drives anti-tumour immunity. *Nature* **575**, 217–223 (2019).
15. Punekar, S. R., Velcheti, V., Neel, B. G. & Wong, K.-K. The current state of the art and future trends in RAS-targeted cancer therapies. *Nat. Rev. Clin. Oncol.* **19**, 637–655 (2022).
16. Dang, C. V., Reddy, E. P., Shokat, K. M. & Soucek, L. Drugging the 'undruggable' cancer targets. *Nat. Rev. Cancer* **17**, 502–508 (2017).

17. Ostrem, J. M. L. & Shokat, K. M. Direct small-molecule inhibitors of KRAS: from structural insights to mechanism-based design. *Nat. Rev. Drug Discov.* **15**, 771–785 (2016).
18. Pant, S. et al. Lymph-node-targeted, mKRAS-specific amphiphile vaccine in pancreatic and colorectal cancer: the phase 1 AMPLIFY-201 trial. *Nat. Med.* **30**, 531–542 (2024).
19. Ostrem, J. M., Peters, U., Sos, M. L., Wells, J. A. & Shokat, K. M. K-Ras(G12C) inhibitors allosterically control GTP affinity and effector interactions. *Nature* **503**, 548–551 (2013).
20. Moore, A. R., Rosenberg, S. C., McCormick, F. & Malek, S. RAS-targeted therapies: is the undruggable drugged?. *Nat. Rev. Drug Discov.* **19**, 533–552 (2020).
21. Wang, X. et al. Identification of MRTX1133, a noncovalent, potent, and selective KRAS inhibitor. *J. Med. Chem.* **65**, 3123–3133 (2022).
22. Mullard, A. Cracking KRAS. *Nat. Rev. Drug Discov.* **18**, 887–891 (2019).
23. Corcoran, R. B. A single inhibitor for all KRAS mutations. *Nat. Cancer* **4**, 1060–1062 (2023).
24. Holderfield, M. et al. Concurrent inhibition of oncogenic and wild-type RAS-GTP for cancer therapy. *Nature* **629**, 919–926 (2024).
25. Thatikonda, V. et al. Co-targeting SOS1 enhances the antitumor effects of KRASG12C inhibitors by addressing intrinsic and acquired resistance. *Nat. Cancer* **5**, 1352–1370 (2024).
26. Ryan, M. B. et al. Vertical pathway inhibition overcomes adaptive feedback resistance to KRASG12C inhibition. *Clin. Cancer Res.* **26**, 1633–1643 (2020).
27. Riedl, J. M. et al. Genomic landscape of clinically acquired resistance alterations in patients treated with KRASG12C inhibitors. *Ann. Oncol.* **36**, 682–692 (2025).
28. Filis, P., Salgkamis, D., Matikas, A. & Zerdes, I. Breakthrough in RAS targeting with pan-RAS(ON) inhibitors RMC-7977 and RMC-6236. *Drug Discov. Today* **30**, 104250 (2025).
29. Jiang, J. et al. Translational and therapeutic evaluation of RAS-GTP inhibition by RMC-6236 in RAS-driven cancers. *Cancer Discov.* **14**, 994–1017 (2024).
30. Gjertsen, M. K. et al. Ex vivo ras peptide vaccination in patients with advanced pancreatic cancer: results of a phase I/II study. *Int. J. Cancer* **65**, 450–453 (1996).
31. Gjertsen, M. K. et al. Intradermal ras peptide vaccination with granulocyte-macrophage colony-stimulating factor as adjuvant: Clinical and immunological responses in patients with pancreatic adenocarcinoma. *Int. J. Cancer* **92**, 441–450 (2001).
32. Zhang, Y., Ma, J.-A., Zhang, H.-X., Jiang, Y.-N. & Luo, W.-H. Cancer vaccines: targeting KRAS-driven cancers. *Expert Rev. Vaccines* **19**, 163–173 (2020).
33. Uprety, D. & Adjei, A. A. KRAS: from undruggable to a druggable Cancer Target. *Cancer Treat. Rev.* **89**, 102070 (2020).
34. Amodio, V. et al. EGFR blockade reverts resistance to KRASG12C inhibition in colorectal cancer. *Cancer Discov.* **10**, 1129–1139 (2020).
35. Ryan, M. B. et al. KRASG12C-independent feedback activation of wild-type RAS constrains KRASG12C inhibitor efficacy. *Cell Rep.* **39**, 110993 (2022).
36. Serebriiskii, I. G. et al. Comprehensive characterization of RAS mutations in colon and rectal cancers in old and young patients. *Nat. Commun.* **10**, 3722 (2019).
37. Levin-Sparenberg, E. et al. A systematic literature review and meta-analysis describing the prevalence of KRAS, NRAS, and BRAF gene mutations in metastatic colorectal cancer. *Gastroenterol. Res.* **13**, 184–198 (2020).
38. Tate, J. G. et al. COSMIC: the catalogue of somatic mutations in cancer. *Nucleic Acids Res.* **47**, D941–D947 (2019).
39. Cerami, E. et al. The cBio cancer genomics portal: an open platform for exploring multidimensional cancer genomics data. *Cancer Discov.* **2**, 401–404 (2012).
40. Giannakis, M. et al. Genomic correlates of immune-cell infiltrates in colorectal carcinoma. *Cell Rep.* **15**, 857–865 (2016).
41. Hoadley, K. A. et al. Cell-of-origin patterns dominate the molecular classification of 10,000 tumors from 33 types of cancer. *Cell* **173**, 291–304.e6 (2018).
42. Yaeger, R. et al. Clinical sequencing defines the genomic landscape of metastatic colorectal cancer. *Cancer Cell* **33**, 125–136.e3 (2018).
43. Knijn, N. et al. KRAS mutation analysis: a comparison between primary tumours and matched liver metastases in 305 colorectal cancer patients. *Br. J. Cancer* **104**, 1020–1026 (2011).
44. Haigis, K. M. KRAS alleles: the devil is in the detail. *Trends Cancer Res.* **3**, 686–697 (2017).
45. Hobbs, G. A., Aaron Hobbs, G. & Der, C. J. RAS mutations are not created equal. *Cancer Discov.* **9**, 696–698 (2019).
46. Woolley, C. E. et al. Coevolution of atypical BRAF and KRAS mutations in colorectal tumorigenesis. *Mol. Cancer Res.***23**, 300–312(2025).
47. Rabara, D. et al. KRAS G13D sensitivity to neurofibromin-mediated GTP hydrolysis. *Proc. Natl Acad. Sci. USA* **116**, 22122 (2019).
48. Jee, J. et al. Automated real-world data integration improves cancer outcome prediction. *Nature* **636**, 728–736 (2024).
49. Vilar, E. & Gruber, S. B. Microsatellite instability in colorectal cancer-the stable evidence. *Nat. Rev. Clin. Oncol.* **7**, 153–162 (2010).
50. Staudacher, J. J. et al. Increased frequency of KRAS mutations in African Americans compared with Caucasians in sporadic colorectal cancer. *Clin. Transl. Gastroenterol.* **8**, e124 (2017).
51. Stolze, B., Reinhart, S., Bulllinger, L., Fröhling, S. & Scholl, C. Comparative analysis of KRAS codon 12, 13, 18, 61, and 117 mutations using human MCF10A isogenic cell lines. *Sci. Rep.* **5**, 8535 (2015).
52. Guerrero, S. et al. K-ras codon 12 mutation induces higher level of resistance to apoptosis and predisposition to anchorage-independent growth than codon 13 mutation or proto-oncogene overexpression. *Cancer Res.* **60**, 6750–6756 (2000).
53. Yoon, H. H. et al. KRAS codon 12 and 13 mutations in relation to disease-free survival in BRAF-wild-type stage III colon cancers from an adjuvant chemotherapy trial (N0147 alliance). *Clin. Cancer Res.* **20**, 3033–3043 (2014).
54. Jones, R. P. et al. Specific mutations in KRAS codon 12 are associated with worse overall survival in patients with advanced and recurrent colorectal cancer. *Br. J. Cancer* **116**, 923–929 (2017).
55. Moretto, R. et al. KRASG12D-mutated metastatic colorectal cancer: Clinical, molecular, immunologic, and prognostic features of a new emerging targeted alteration. *JCO Precis. Oncol.* **8**, e2400329 (2024).
56. Hirose, T. et al. A retrospective analysis of the prognostic impact of *KRAS* G12D mutation in patients with *RAS*-mutated metastatic colorectal cancer. *J. Clin. Oncol.* **42**, 105–105 (2024).
57. Imamura, Y. et al. Analyses of clinicopathological, molecular, and prognostic associations of KRAS codon 61 and codon 146 mutations in colorectal cancer: cohort study and literature review. *Mol. Cancer* **13**, 135 (2014).
58. Smith, G. et al. Activating K-Ras mutations outwith 'hotspot' codons in sporadic colorectal tumours—implications for personalised cancer medicine. *Br. J. Cancer* **102**, 693–703 (2010).
59. Loupakis, F. et al. KRAS codon 61, 146 and BRAF mutations predict resistance to cetuximab plus irinotecan in KRAS codon 12 and 13 wild-type metastatic colorectal cancer. *Br. J. Cancer* **101**, 715–721 (2009).
60. Poulin, E. J. et al. Tissue-specific oncogenic activity of KRAS A146T. *Cancer Discov.* **9**, 738–755 (2019).
61. De Roock, W. et al. Effects of KRAS, BRAF, NRAS, and PIK3CA mutations on the efficacy of cetuximab plus chemotherapy in chemotherapy-refractory metastatic colorectal cancer: a retrospective consortium analysis. *Lancet Oncol.* **11**, 753–762 (2010).
62. Douillard, J.-Y. et al. Panitumumab-FOLFOX4 treatment and RAS mutations in colorectal cancer. *N. Engl. J. Med.* **369**, 1023–1034 (2013).
63. Center for Drug Evaluation & Research. FDA grants accelerated approval to adagrasib with cetuximab for KRAS G12C-mutated colorectal cancer. *U.S. Food and Drug Administration* https://www.

fda.gov/drugs/resources-information-approved-drugs/fda-grants-accelerated-approval-adagrasib-cetuximab-kras-g12c-mutated-colorectal-cancer (2024).
64. Center for Drug Evaluation & Research. FDA approves sotorasib with panitumumab for KRAS G12C-mutated colorectal cancer. *U.S. Food and Drug Administration* https://www.fda.gov/drugs/resources-information-approved-drugs/fda-approves-sotorasib-panitumumab-kras-g12c-mutated-colorectal-cancer (2025).
65. Gao, J. et al. Integrative analysis of complex cancer genomics and clinical profiles using the cBioPortal. *Sci. Signal.* **6**, l1 (2013).
66. Xu, S. et al. Structural insight into the rearrangement of the switch I region in GTP-bound G12A K-Ras. *Acta Crystallogr D. Struct. Biol.* **73**, 970–984 (2017).
67. Berman, H. M. The Protein Data Bank. *Nucleic Acids Res*. **28**, 235–242 (2000).
68. Sehnal, D. et al. Mol* Viewer: modern web app for 3D visualization and analysis of large biomolecular structures. *Nucleic Acids Res.* **49**, W431–W437 (2021).
69. R Core Team. R: A Language and Environment for Statistical Computing. R Foundation for Statistical Computing, Vienna, Austria. https://www.R-project.org/ (2024).
70. Kim, S. et al. PubChem 2023 update. *Nucleic Acids Res.* **51**, D1373–D1380 (2023).

Acknowledgements

The authors sincerely thank Francisco Javier Perez Vicente, head of the IGTP Scientific Computing Facility. The authors used generative AI (Microsoft Copilot) solely to assist with grammar and style editing using the prompt 'revise grammar and fluency'. The scientific content, analysis, and conclusions were entirely generated by the authors. SA has received grants from the Fundación Mutua Madrileña (AP174232020) and Instituto de Salud Carlos III, Spanish Ministry of Science, Innovation and Universities (FIS PI21/01766) (co-funded by the European Regional Development Fund, "A way to make Europe"). NM has received grants from SEOM (Sociedad Española de Oncología Médica - Proyectos de Investigación 2024), Fundació Olga Torres (Beca Dionís Torres Segura 2024), and Instituto de Salud Carlos III, Spanish Ministry of Science, Innovation and Universities (FIS PI24/00824).

Author contributions

M.N.J., B.G., and S.A. conducted the literature review on KRAS mutations in colorectal cancer and current inhibitors. N.M. and C.H. contributed their clinical expertise by reviewing the literature, curating clinical trials information, and drafting the sections on clinical challenges and patient management. S.A. performed the computational and statistical analyses. M.N.J., B.G., and S.A. jointly interpreted the results and prepared the figures. All authors contributed to the writing, revision, and approval of the final version of the manuscript.

Competing interests

Maria Navarro is currently an employee of Ability Pharmaceuticals, Cerdanyola del Vallès, Barcelona, Spain. She contributed to this work while she was a member of the Cancer Genetics and Epigenetics Laboratory at the IGTP. Cinta Hierro received honoraria (as invited speaker or consultant) from Lilly, MSD, BMS, AstraZeneca, Astellas and JAZZ Pharmaceuticals, and has received research funding via the Institution from Merck. She has participated as principal investigator in clinical trials (unrelated to this work) from BMS, MSD, ALX Oncology, JAZZ Pharmaceuticals, AstraZeneca, Abbie, Relay Therapeutics and Medicenna Therapeutics. She has also received travel fees from BMS, MSD, Roche, Amgen, AstraZeneca and Merck. Nuria Mulet has served in an Advisory Role for Amgen and has received travel grants from Merck and MSD. None of the listed companies or funding agencies was involved in the study design, data acquisition, analysis, interpretation of results, or manuscript preparation. The authors declare that this research was conducted independently and without any commercial, intellectual, or financial relationships with any commercial entity.

Consent to participate

The study does not involve human donors or animal models.

Consent for publication

All authors have read and agreed to the published version of the manuscript.

Additional information

Supplementary information The online version contains supplementary material available at https://doi.org/10.1038/s41698-025-01166-3.

Correspondence and requests for materials should be addressed to Sergio Alonso.